

Strengthened and Faster Linear Approximation to Joint Chance Constraints with Wasserstein Ambiguity

Yihong Zhou

School of Engineering, University of Edinburgh, U.K., yihong.zhou@ed.ac.uk,

Yuxin Xia

School of Engineering, University of Edinburgh, U.K., yuxin.xia@ed.ac.uk,

Hanbin Yang

School of Data Science, The Chinese University of Hong Kong, Shenzhen, China, hanbinyang@link.cuhk.edu.cn,

Thomas Morstyn

Department of Engineering Science, University of Oxford, U.K., thomas.morstyn@eng.ox.ac.uk,

Many real-world decision-making problems in energy systems, transportation, and finance have uncertain parameters in their constraints. Wasserstein distributionally robust joint chance constraints (WDRJCC) offer a promising solution by explicitly guaranteeing the probability of the simultaneous satisfaction of multiple constraints in a robust manner. WDRJCC are computationally demanding, and although manageable for small problems, practical applications often demand more tractable approaches—especially for large-scale and complex problems, such as power system unit commitment problems and multilevel problems with chance constraints in lower levels. To address this, this paper proposes a novel inner-approximation for a specific type of WDRJCC, namely WDRJCC with right-hand-side uncertainties (RHS-WDRJCC). Motivated by the strengthening process that leads to a faster but still exact mixed-integer reformulation to RHS-WDRJCC, we propose a Strengthened and Faster Linear Approximation (SFLA) by strengthening an existing convex inner-approximation that is equivalent to the worst-case conditional value-at-risk (W-CVaR) method under specific hyperparameters. This strengthening process reduces the number of constraints and tightens the feasible region for ancillary variables, leading to significant computational speedup. Despite the tightening, we prove that the proposed SFLA does not introduce additional conservativeness and can even lead to less conservativeness. The significance and superiority of the proposed SFLA are numerically validated in two important real-world problems. In a power system unit commitment problem, the proposed SFLA achieves up to 10× and on average 3.8× computational speedup compared to the strengthened and exact mixed-integer reformulation in finding comparable high-quality feasible solutions. In a bilevel strategic bidding problem where the exact reformulation is not applicable due to non-convexity, we show that the proposed SFLA can lead to 90× speedup compared to existing convex approximation methods such as W-CVaR.

Key words: Faster linear approximation, Wasserstein distributionally robust joint chance constraints, conditional value-at-risk

1. Introduction

Many real-world decision-making problems in energy systems, transportation, and finance involve constraints with uncertain parameters due to variable supply, customer demand, and economic conditions (Gabrel et al. 2014). A typical solution approach is robust optimization (RO), which

aims to ensure feasibility for each possible scenario; however, this often leads to overly conservative solutions. In contrast, chance-constrained programming (CCP) provides a less restrictive alternative (Prékopa 2013). CCP supports robust but economic decision-making by explicitly limiting the probability of constraint violations, allowing for a controlled degree of conservativeness relative to RO. As a result, CCP has found widespread applications in fields such as power systems, economics, finance, and water management (Geng and Xie 2019).

However, classic CCP models are based on the exact distribution of random variables, which is typically not available, and decision-makers generally only possess a historical dataset. This dataset may be insufficient to accurately infer the true distribution of random variables, which limits the out-of-sample performances of a CCP model. To hedge the ambiguity of the underlying distribution, distributionally robust chance-constrained programming (DRCCP) has been proposed to control the violation probability under the worst-case probability distribution over a so-called ‘‘ambiguity’’ set (Scarf et al. 1957). This ambiguity set may be defined as the set of probability distributions with the same statistic moments such as mean and variance (Delage and Ye 2010), or defined as distributions within a certain distance from the reference distribution. Despite good tractability, moment-based ambiguity sets do not fully use the information of the datasets and may lead to over-conservativeness (Gao and Kleywegt 2023). For distance-based ambiguity sets, the Wasserstein distance is widely applied due to its good out-of-sample performance (Mohajerin Esfahani and Kuhn 2018), and the advantage of Wasserstein-based ambiguity sets over other distance-based sets was discussed by Gao and Kleywegt (2023). A Wasserstein DRCCP model can be written as:

$$\min_{\mathbf{x} \in \mathcal{X}} c(\mathbf{x}) \quad (1a)$$

$$\text{s.t.} \quad \sup_{\mathbb{P} \in \mathcal{F}_N(\theta)} \mathbb{P}[\boldsymbol{\xi} \notin \mathcal{S}(\mathbf{x})] \leq \epsilon, \quad (1b)$$

where $c(\cdot)$ is the objective function, $\mathcal{X} \subset \mathbb{R}^L$ is a compact domain for the decision variables $\mathbf{x} \in \mathbb{R}^L$. Constraint (1b) ensures that the random vector $\boldsymbol{\xi} \subseteq \mathbb{R}^K$ falls outside the decision-dependent safety set $\mathcal{S}(\mathbf{x})$ with a small probability, which is not greater than the risk level ϵ under the worst-case distribution $\mathbb{P} \in \mathcal{F}_N(\theta)$. Here, the Wasserstein ambiguity set $\mathcal{F}(\theta)$ is defined as a ball with radius θ centered at the empirical distribution \mathbb{P}_N constructed by historical data:

$$\mathcal{F}_N(\theta) := \{\mathbb{P} \mid d_W(\mathbb{P}_N, \mathbb{P}) \leq \theta\}. \quad (2)$$

Following Chen et al. (2022) and Ho-Nguyen et al. (2021), we consider the 1-Wasserstein distance based on a general norm $\|\cdot\|$:

$$d_W(\mathbb{P}, \mathbb{P}') := \inf_{\Pi \in \mathcal{P}(\mathbb{P}, \mathbb{P}')} \mathbb{E}_{(\xi, \xi') \sim \Pi} [\|\xi - \xi'\|], \quad (3)$$

where $\mathcal{P}(\mathbb{P}, \mathbb{P}')$ is a set of distributions with marginal distributions \mathbb{P} and \mathbb{P}' . This paper focuses on Wasserstein distributionally robust joint chance constraints under right-hand-side uncertainty (RHS-WDRJCC) (1b) with the following safety set:

$$\mathcal{S}(\mathbf{x}) := \{\xi \mid \mathbf{a}_p^\top \mathbf{x} \leq \mathbf{b}_p^\top \xi + d_p, p \in [P]\}, \quad (4)$$

where there are P constraints indexed by $[P] := \{1, \dots, P\}$ that need to be met jointly with high probability $1 - \epsilon$ with $\epsilon \in (0, 1)$. This joint satisfaction is desired in practical applications for its higher safety (Geng and Xie 2019, Ding et al. 2022), and the RHS uncertainty also arises in several practical problems, such as managing the thermal constraints of the power grid lines, securing the power system reserve (Wang et al. 2016, Wu et al. 2016, Yang et al. 2020), or restricting the load-generation imbalance (van Ackooij et al. 2018).

To exactly solve the problem with RHS-WDRJCC (1), Chen et al. (2022) proposed an exact mixed-integer programming (MIP) reformulation, which was further strengthened by Ho-Nguyen et al. (2021) by exploiting valid inequalities and reducing the values of big-M. Jiang and Xie (2024b) further proposed a method that combines inner and outer approximations to derive optimality cuts, thereby accelerating the exact MIP solution process. Alternative methods include ALSO-X, ALSO-X+, and ALSO-X# that (approximately) solve a CCP in an iterative way with high quality (Jiang and Xie 2022, 2024a). However, the MIP-based exact reformulation is NP-hard, and these ALSO methods may have numerical issues and lack of stability due to their iterative schemes. Greater tractability is still desired, especially when the original deterministic problem is already complicated. We have identified two types of practical applications that necessitate more computationally efficient solution schemes.

One typical example is the power system unit commitment (UC) problem that determines the on/off statuses of generators to minimize operational cost within power network constraints, which is a large-scale multi-period MIP problem with thousands of generators and network nodes included. In one of the largest electricity markets in the world, managed by the Midcontinent Independent System Operator (MISO), the network model includes more than 45000 buses, 1400 generation sources, around 2500 pricing nodes, and has a 36-hour look-ahead horizon with hourly resolution

(Chen et al. 2016, Sun et al. 2018). Additionally, UC problems may be solved repeatedly during the market clearing process to accommodate necessary modifications to constraints or other evaluations. Moreover, the entire process must be completed within a stringent time frame of three to four hours (Chen et al. 2016). The UC complexity is further exacerbated by the increasing number of virtual bids (bids for speculation submitted by purely financial players with no obligation to own physical generation) and the increasing number of combined cycle units that require complicated operation models (Sun et al. 2018). However, the increasing penetration of fluctuating renewables increases the uncertainty level of the system, and thus it becomes more important to have chance-constrained UC to ensure reliable operation (Yang et al. 2020, van Ackooij et al. 2018).

The second example involves applying RHS-WDRJCC at lower levels of bilevel or multilevel optimization problems, where all levels need to reach optimum. To solve these multilevel problems, Karush-Kuhn-Tucker (KKT) conditions or strong duality need to be exploited to derive solvable single-level counterparts, which require convexity in lower levels. Practical applications include strategic price-maker bidders in day-ahead energy markets (Paredes et al. 2023) and gas markets that involve a sequential clearing process (Heitsch et al. 2022). In these applications, market clearing is modeled at lower levels. Because the clearing process can occur before uncertainties are revealed (e.g., day-ahead markets), a CCP needs to be implemented at these lower levels to manage uncertainties (Beck et al. 2023). However, the MIP-based RHS-WDRJCC reformulation (Ho-Nguyen et al. 2021) is unsuitable due to its non-convexity, and the iterative ALSO methods (Jiang and Xie 2022, 2024a) are less capable of incorporating optimality conditions.

Due to the high complexity of these practical problems, it is desirable to have convex or linear approximations of RHS-WDRJCC, so as to bring a minimum extra computational effort while maintaining solution quality. Common approaches include the Bonferroni approximation (Chen et al. 2023), which can become overly conservative when events overlap significantly, and the worst-case conditional value at risk (W-CVaR) (Mohajerin Esfahani and Kuhn 2018, Chen et al. 2023), a common approximation for CCPs. Chen et al. (2023) also introduced the “best” convex inner-approximation for RHS-WDRJCC, which is equivalent to W-CVaR under certain hyperparameters. However, these approximation schemes introduce a large number of additional ancillary variables and constraints, which brings excessive computing burden, especially for the UC and multilevel problems discussed above; consequently, CCPs generally remain unscalable for industrial-scale instances (Zhao et al. 2024). Therefore, it is still preferable to further enhancing computational efficiency of RHS-WDRJCC.

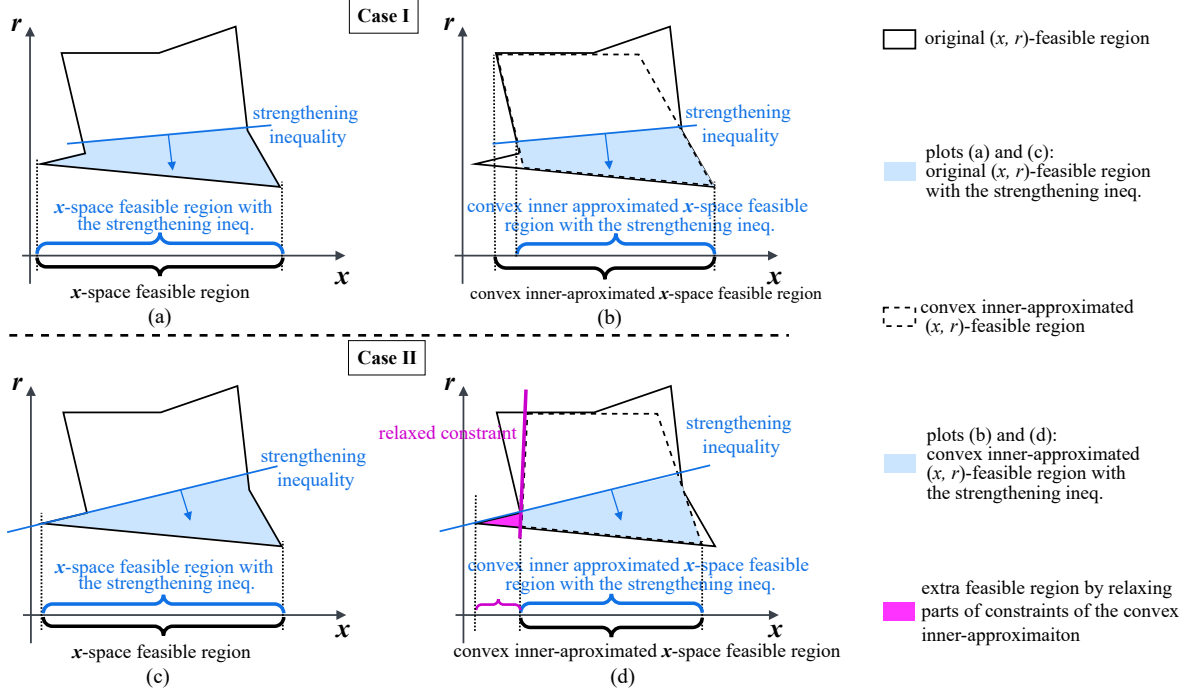


Figure 1 Two possible cases when a strengthening inequality valid for the original feasible region is applied to the convex inner-approximation.

Note. Analytical reformulations sometimes (such as for WDRJCC) introduce ancillary variable r in addition to the original decision variable x . Case I: A strengthening inequality is valid for the original nonconvex region but leads to higher conservativeness to its inner-approximation. (a) In the original nonconvex feasible region of x and r , the strengthening (valid) inequality excludes a redundant portion without reducing the feasible region of x . (b) The convex inner-approximation (dashed) has a smaller feasible region of x compared to the original region, and the strengthening inequality further reduces the x feasible region, resulting in even higher conservativeness. Case II: A strengthening inequality is valid for both the original nonconvex region and its inner-approximation. (c) In the original nonconvex feasible region, the strengthening inequality excludes a redundant portion without reducing the feasible region of x . (d) The convex inner-approximation (dashed) has a smaller feasible region of x compared to the original region, and the strengthening inequality does not further reduce the x feasible region. Furthermore, by relaxing certain constraints of the convex inner-approximation, it is possible to include an extra non-empty feasible region (depicted in purple) and thus expand the feasible region of x (less conservativeness). This extra feasible region is small relative to the excluded region; therefore, the overall search space is still reduced, preserving the computational efficiency provided by the strengthening inequality.

One promising solution approach is utilizing valid inequalities, which are additional constraints introduced to an optimization problem to tighten the formulation without excluding any feasible solutions from the original problem's feasible region. Motivated by the work of Ho-Nguyen et al. (2021) where valid inequalities were exploited to strengthen the exact MIP reformulation so as to speed up computation, this paper shows that the strengthening process can also be migrated to a convex inner-approximation that admits W-CVaR equivalence. This migration reduces the number of constraints in the original convex approximation and tighten the feasible region for ancillary variables, which leads to significant computational speedups. It is worth noting that the migration

of a strengthening process can introduce higher conservativeness to a convex inner-approximation, as shown in Case I of Figure 1. However, we prove that the proposed SFLA will always lead to Case II in Figure 1, which does not introduce additional conservativeness and can even produce a less conservative inner-approximation. The computational speedup and reduced conservativeness of the proposed SFLA address the practical needs of industry-scale problems, such as UC and bilevel strategic bidding. In summary, the main contributions of this paper include:

- (1) We proposed a Strengthened and Faster Linear Approximation (SFLA) to RHS-WDRJCC. By exploiting valid inequalities for a convex inner-approximation that is equivalent to W-CVaR (Chen et al. 2023) under specific hyperparameters, the number of constraints are reduced and the feasible region of ancillary variables are tightened, which leads to significant computational speedup. Even with the tightening, we prove that the proposed SFLA does not introduce additional conservativeness and can even provide a less conservative inner-approximation. In addition, we offer theoretical guidance for setting the SFLA hyperparameter and analyze when SFLA becomes equivalent to exact reformulation or equivalent to existing linear approximations such as W-CVaR.
- (2) We demonstrated the superiority of the proposed SFLA through extensive numerical studies on two important real-world large-scale chance-constrained optimization problems. First, in the UC problem, the proposed SFLA achieves up to $10\times$ and on average $3.8\times$ computational speedup compared to the existing strengthened and exact MIP reformulation (Ho-Nguyen et al. 2021) in finding comparable high-quality solutions. We also demonstrate that the proposed SFLA achieves approximation quality comparable to the exact reformulation, except for minor inferiority only occurring under the combination of a high risk level, a large number of historical data, and a small ambiguity set radius. Second, in the bilevel strategic bidding problem where the exact formulation is not applicable due to non-convexity, the proposed SFLA demonstrates $90\times$ speedup in computation time compared to convex inner-approximations such as W-CVaR.

This paper is organized as follows. Section 2 lists the existing exact reformulation and convex inner-approximations. Section 3 introduces the proposed SFLA and proves its relationship to the exact reformulation and other convex approximations. Section 4 carries out numerical studies and Section 5 concludes this paper.

2. Problem Formulation

This paper focuses on RHS-WDRJCC (1b), with the safety set described in Eq. (4). In what follows, we assume $\epsilon \in (0, 1)$ and $\theta > 0$, which are conditions necessary for the subsequent exact

reformulation on which this work is based (Chen et al. 2022). This section summarizes the current exact reformulation and approximation methods for RHS-WDRJCC.

2.1. Exact Reformulation

Suppose we have collected N independent and identically distributed (i.i.d.) samples $\{\xi_i\}_{i \in [N]}$ for the random vector ξ , where the index set is defined as $[N] := \{1, \dots, N\}$. Given a decision $\mathbf{x} \in \mathcal{X}$ and a sample ξ_i , we define the distance from ξ_i to the complement of $\mathcal{S}(\mathbf{x})$ as:

$$\text{dist}(\xi_i, \mathcal{S}(\mathbf{x})) = \inf_{\xi' \in \mathbb{R}^K} \{\|\xi_i - \xi'\| \mid \xi' \notin \mathcal{S}(\mathbf{x})\}. \quad (5)$$

Building on the results given by Chen et al. (2022) and the safety set defined in (4), we can reformulate $\text{dist}(\xi_i, \mathcal{S}(\mathbf{x}))$ to the following analytical expression:

$$\text{dist}(\xi_i, \mathcal{S}(\mathbf{x})) = \left(\min_{p \in [P]} \frac{\mathbf{b}_p^\top \xi_i + d_p - \mathbf{a}_p^\top \mathbf{x}}{\|\mathbf{b}_p\|_*} \right)^+ = \min_{p \in [P]} \left(\frac{\mathbf{b}_p^\top \xi_i + d_p - \mathbf{a}_p^\top \mathbf{x}}{\|\mathbf{b}_p\|_*} \right)^+, \quad (6)$$

where $\|\cdot\|_*$ is the dual norm and $(\cdot)^+$ extracts the non-negative component of the argument, setting negative values to zero. By introducing ancillary variables $s \in \mathbb{R}$ and $\mathbf{r} \in \mathbb{R}^P$, Chen et al. (2022) showed that RHS-WDRJCC (1b) can be expressed as the following distance-based formulation:

$$s \geq 0, \mathbf{r} \geq \mathbf{0}, \quad (7a)$$

$$\epsilon N s - \sum_{i=1}^N r_i \geq \theta N, \quad (7b)$$

$$\left(\frac{\mathbf{b}_p^\top \xi_i + d_p - \mathbf{a}_p^\top \mathbf{x}}{\|\mathbf{b}_p\|_*} \right)^+ \geq s - r_i, \quad \forall i \in [N], p \in [P]. \quad (7c)$$

While this distance-based formulation cannot be directly processed by commercial solvers such as Gurobi (Gurobi Optimization, LLC 2024), it can be transformed into an equivalent MIP formulation:

$$\mathbf{z} \in \{0, 1\}^N, s \geq 0, \mathbf{r} \geq \mathbf{0}, \quad (8a)$$

$$\epsilon N s - \sum_{i=1}^N r_i \geq \theta N, \quad (8b)$$

$$M(1 - z_i) \geq s - r_i, \quad \forall i \in [N], \quad (8c)$$

$$\frac{\mathbf{b}_p^\top \xi_i + d_p - \mathbf{a}_p^\top \mathbf{x}}{\|\mathbf{b}_p\|_*} + M z_i \geq s - r_i, \quad \forall i \in [N], p \in [P]. \quad (8d)$$

This MIP reformulation, based on Chen et al. (2022), is originally designed for open safety sets, but Ho-Nguyen et al. (2021) demonstrated that it applies to both open and closed sets.

Despite being solvable by advanced MIP solvers, MIP reformulation remains NP-hard and its complexity becomes particularly problematic when the original deterministic problem is already complicated or requires convexity for tractable reformulation such as in multilevel problems. Therefore, this paper focuses on convex inner-approximation (for safety) of the \mathbf{x} -feasible region $\mathcal{X}_{\text{Exact}}$, which is defined by the RHS-WDRJCC in (1) for the original decision variable \mathbf{x} :

$$\mathcal{X}_{\text{Exact}} := \{\mathbf{x} \in \mathcal{X} \mid \exists s, \mathbf{r} : (7a)-(7c)\}, \quad (9)$$

because this is the region that affects the objective value $c(\mathbf{x})$ in (1a).

2.2. Convex Inner-Approximations

In this section, we introduce three representative convex inner-approximation methods for RHS-WDRJCC. The first is the Bonferroni approximation, which is a straightforward and computationally efficient inner-approximation that replaces a joint chance constraint (JCC) with individual chance constraints at reduced individual risk levels ϵ_p . According to Chen et al. (2023), the Bonferroni approximation of RHS-WDRJCC (1b) can be formulated as:

$$\mathbf{a}_p^\top \mathbf{x} \leq d_p - \sup_{\mathbb{P} \in \mathcal{F}(\theta)} \mathbb{P}\text{-VaR}_{\epsilon_p}(-\mathbf{b}_p^\top \tilde{\boldsymbol{\xi}}), \quad \forall p \in [P], \quad (10)$$

where the preset individual risk levels ϵ_p must satisfy $\sum_{p \in P} \epsilon_p \leq \epsilon$. Here, $\sup_{\mathbb{P} \in \mathcal{F}(\theta)} \mathbb{P}\text{-VaR}_{\epsilon_p}(-\mathbf{b}_p^\top \tilde{\boldsymbol{\xi}})$ is the optimal value of the following bilinear optimization problem:

$$\min_{\alpha, \beta, \mathbf{m}, \eta} \quad \eta \quad (11a)$$

$$\text{s.t.} \quad \theta\beta + \frac{1}{N} \sum_{i=1}^N \alpha_i \leq \epsilon_p, \quad (11b)$$

$$\alpha_i \geq 1 - m_i(\eta + \mathbf{b}_p^\top \boldsymbol{\xi}_i), \quad \forall i \in [N], \quad (11c)$$

$$\beta \geq m_i \|\mathbf{b}_p\|_*, \quad \forall i \in [N], \quad (11d)$$

$$\alpha \geq 0, \quad \mathbf{m} \geq 0, \quad (11e)$$

which captures the risk of constraint violation under distributional uncertainty within a θ -radius Wasserstein ball and can be solved by a line search along η or bilinear solvers. Problem (11) is solved first, and the optimal value, namely $\sup_{\mathbb{P} \in \mathcal{F}(\theta)} \mathbb{P}\text{-VaR}_{\epsilon_p}(-\mathbf{b}_p^\top \tilde{\boldsymbol{\xi}})$, serves as parameters for the Bonferroni approximation (10).

The Bonferroni approximation (10) does not add extra variables or constraints to the original deterministic problem, resulting in minimal computational overhead. A common practice is to set $\epsilon_p = \epsilon/P$ (Geng and Xie 2019), but this often leads to excessive conservativeness, especially when P is large or when the safety constraints are correlated (Chen et al. 2007). However, even with optimized ϵ_p , the approach can still be overly conservative in some cases, and finding optimal values for ϵ_p is generally intractable (Chen et al. 2023). As will be shown in our case studies, the Bonferroni approximation often leads to infeasibility due to this conservativeness. Consequently, we exclude this approach from theoretical comparisons in the following discussion.

An alternative and widely applied inner-approximation is W-CVaR (Mohajerin Esfahani and Kuhn 2018, Chen et al. 2023), which can be formulated as the following set of linear constraints:

$$\boldsymbol{\alpha} \geq \mathbf{0}, \beta \in \mathbb{R}, \tau \in \mathbb{R}, \quad (12a)$$

$$\tau + \frac{1}{\epsilon} \left(\theta\beta + \frac{1}{N} \sum_{i \in [N]} \alpha_i \right) \leq 0, \quad (12b)$$

$$\alpha_i \geq w_p \left(\mathbf{a}_p^\top \mathbf{x} - \mathbf{b}_p^\top \boldsymbol{\xi}_i - d_p \right) - \tau, \quad \forall i \in [N], p \in [P], \quad (12c)$$

$$\beta \geq w_p \|\mathbf{b}_p\|_*, \quad \forall p \in [P], \quad (12d)$$

where $\mathbf{w} := [w_p]_{p \in [P]}$ subject to $\mathbf{w} \in \Delta_{++} := \{\mathbf{w} \in (0, 1)^P : \sum_{p \in [P]} w_p = 1\}$ is a tunable hyperparameter that affects the performance of the W-CVaR approximation by prioritizing specific constraints in $\mathcal{S}(\mathbf{x})$ (Chen et al. 2023, Ordoudis et al. 2021). Similarly, we define its \mathbf{x} -feasible region as:

$$\mathcal{X}_{\text{WCVaR}}(\mathbf{w}) := \{\mathbf{x} \in \mathcal{X} \mid \exists \boldsymbol{\alpha}, \beta, \tau : (12a)-(12d)\}. \quad (13)$$

Another convex approximation (Chen et al. 2023) reformulates the exact RHS-WDRJCC (7) by overcoming the non-convexity caused by the distance function (6). More specifically, this approximation method replaces the original distance function $\text{dist}(\boldsymbol{\xi}_i, \mathcal{S}(\mathbf{x}))$ with a conservative approximation $\widehat{\text{dist}}(\boldsymbol{\xi}_i, \mathcal{S}(\mathbf{x}))$ given by:

$$\widehat{\text{dist}}(\boldsymbol{\xi}_i, \mathcal{S}(\mathbf{x})) := \kappa_i \left(\min_{p \in [P]} \frac{\mathbf{b}_p^\top \boldsymbol{\xi}_i + d_p - \mathbf{a}_p^\top \mathbf{x}}{\|\mathbf{b}_p\|_*} \right), \quad (14)$$

where $\kappa_i \in [0, 1]$ are pre-selected parameters. Since $\widehat{\text{dist}}(\boldsymbol{\xi}_i, \mathcal{S}(\mathbf{x})) \leq \text{dist}(\boldsymbol{\xi}_i, \mathcal{S}(\mathbf{x}))$, the replacement yields the following linear inner-approximation (LA) of the constraints in (7):

$$s \geq 0, \mathbf{r} \geq \mathbf{0}, \quad (15a)$$

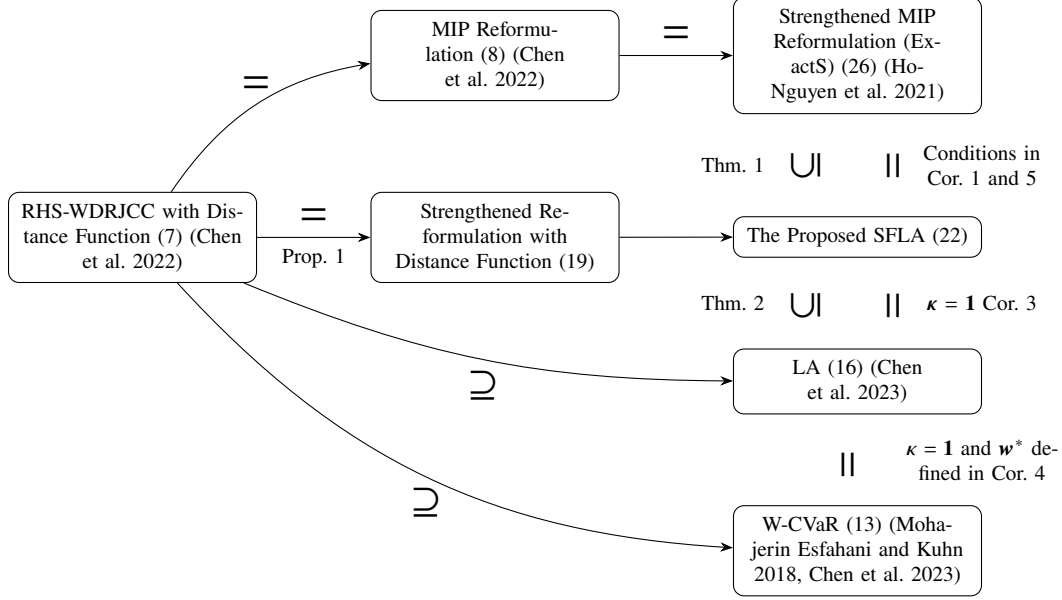


Figure 2 The derivation flow and the formulation comparisons of the x -feasible region defined by different reformulation of RHS-WDRJCC.

$$\epsilon N s - \sum_{i \in [N]} r_i \geq \theta N, \quad (15b)$$

$$\kappa_i \left(\frac{\mathbf{b}_p^\top \boldsymbol{\xi}_i + d_p - \mathbf{a}_p^\top \mathbf{x}}{\|\mathbf{b}_p\|_*} \right) \geq s - r_i, \quad \forall i \in [N], p \in [P]. \quad (15c)$$

Chen et al. (2023) showed that LA (15) represents a family of the “best” inner-approximation in the $(\mathbf{x}, s, \mathbf{r})$ -feasible region of (7) and LA (15) becomes exact by optimizing $\boldsymbol{\kappa} := [\kappa_i]_{i \in [N]}$. Furthermore, as demonstrated by Chen et al. (2023), LA (15) with $\boldsymbol{\kappa} = \mathbf{1}$ is equivalent to W-CVaR for a specific setting of \mathbf{w} , and becomes exact under certain conditions. These conditions are also extended to our proposed approximation as will be illustrated in Corollaries 4 and 5. The x -feasible region of the LA approximation can be expressed as:

$$\mathcal{X}_{\text{LA}}(\boldsymbol{\kappa}) = \{\mathbf{x} \in \mathcal{X} \mid \exists s, \mathbf{r} : (15a)–(15c)\}. \quad (16)$$

3. Strengthened and Faster Linear Approximation

Our proposed approximation is motivated by the strengthening of the exact MIP reformulation. As discussed, the RHS-WDRJCC reformulation (7) can be exactly reformulated as a set of MIP constraints in (8). Ho-Nguyen et al. (2021) showed that the MIP (8) can be further strengthened to another exact MIP reformulation (denoted by ExactS), by replacing $NP - \lfloor \epsilon N \rfloor P$ constraints with P valid inequalities. For convenience, the formulation of ExactS is reproduced as Eq. (25) in Appendix A. The x -feasible region of ExactS remains equivalent to the exact MIP set (8), but the

number of constraints and the complexity of the whole $(\mathbf{x}, s, \mathbf{r})$ -feasible region are reduced. In this section, we will show that this strengthening procedure can be migrated to the RHS-WDRJCC (7) expressed by the distance function (Proposition 1), which then enables the derivation of our proposed approximation, termed as *Strengthened and Faster Linear Approximation* (SFLA). Finally, rather than compromising the \mathbf{x} -feasible region as illustrated in Case I of Figure 1, we prove that the proposed SFLA is always the Case II: the proposed SFLA will not introduce extra conservativeness and can even be less conservative than LA proposed by Chen et al. (2023) (Theorem 2). Figure 2 displays the derivation process and a comparison of different formulations in the \mathbf{x} -feasible region.

3.1. Derivation and Formulation

Let $k := \lfloor \epsilon N \rfloor$ and assume an ordering $\mathbf{b}_p^\top \boldsymbol{\xi}_1 \leq \dots \leq \mathbf{b}_p^\top \boldsymbol{\xi}_N$ without loss of generality. We further denote by q_p the $(k+1)$ -th smallest value as:

$$q_p := \mathbf{b}_p^\top \boldsymbol{\xi}_{k+1}. \quad (17)$$

Then we introduce the index set $[N]_p$ with only $k = \lfloor \epsilon N \rfloor$ elements as:

$$[N]_p := \{i \in [N] \mid \mathbf{b}_p^\top \boldsymbol{\xi}_i < q_p\}, \quad \forall p \in [P]. \quad (18)$$

In addition, we introduce the following lemma:

LEMMA 1 (Lemma 1 in Ho-Nguyen et al. (2021)). *For any fixed $\mathbf{x} \in \mathcal{X}_{Exact}$, there exists (\mathbf{r}, s) such that s is equal to the $(k+1)$ -th smallest value amongst $\{\text{dist}(\boldsymbol{\xi}_i, \mathcal{S}(\mathbf{x}))\}_{i \in [N]}$ and constraints (7a)–(7c) are satisfied.*

With Lemma 1, we propose the following proposition which demonstrates that the strengthening procedures for the exact MIP reformulation (8) in Ho-Nguyen et al. (2021) can be migrated to the exact RHS-WDRJCC reformulation (7) expressed by the distance function $\text{dist}(\boldsymbol{\xi}_i, \mathcal{S}(\mathbf{x}))$.

PROPOSITION 1. *The feasible set \mathcal{X}_{Exact} (9) can be equivalently defined by the following set of strengthened constraints, by replacing $NP - \lfloor \epsilon N \rfloor P$ constraints in (7c) involving the distance function with P valid inequalities (19d) and only keeping $\lfloor \epsilon N \rfloor P$ constraints in (7c) as (19c):*

$$s \geq 0, \mathbf{r} \geq \mathbf{0}, \quad (19a)$$

$$\epsilon N s - \sum_{i \in [N]} r_i \geq \theta N, \quad (19b)$$

$$\left(\frac{\mathbf{b}_p^\top \boldsymbol{\xi}_i + d_p - \mathbf{a}_p^\top \mathbf{x}}{\|\mathbf{b}_p\|_*} \right)^+ \geq s - r_i, \quad \forall i \in [N]_p, p \in [P], \quad (19c)$$

$$\frac{q_p + d_p - \mathbf{a}_p^\top \mathbf{x}}{\|\mathbf{b}_p\|_*} \geq s, \quad \forall p \in [P]. \quad (19d)$$

In other words, we have:

$$\mathcal{X}_{Exact} = \{\mathbf{x} \in \mathcal{X} \mid \exists s, \mathbf{r} : (19a)-(19d)\}. \quad (20)$$

The proof of Proposition 1 is provided in Appendix B. The form of constraints in (19) motivates us to propose SFLA, by replacing the non-convex constraints (19c) with the approximated distance function $\widehat{\text{dist}}(\boldsymbol{\xi}_i, \mathcal{S}(\mathbf{x}))$ introduced in Eq. (14), while keeping the the strengthening structure in (19). Therefore, the proposed SFLA can be expressed as:

$$s \geq 0, \mathbf{r} \geq \mathbf{0}, \quad (21a)$$

$$\epsilon N s - \sum_{i \in [N]} r_i \geq \theta N, \quad (21b)$$

$$\kappa_i \left(\frac{\mathbf{b}_p^\top \boldsymbol{\xi}_i + d_p - \mathbf{a}_p^\top \mathbf{x}}{\|\mathbf{b}_p\|_*} \right) \geq s - r_i, \quad \forall i \in [N]_p, p \in [P], \quad (21c)$$

$$\frac{q_p + d_p - \mathbf{a}_p^\top \mathbf{x}}{\|\mathbf{b}_p\|_*} \geq s, \quad \forall p \in [P]. \quad (21d)$$

where we still have the preset hyperparameters $\kappa_i \in [0, 1]$ for all $i \in [N]$. The \mathbf{x} -feasible region of the proposed SFLA can be expressed as:

$$\mathcal{X}_{SFLA}(\boldsymbol{\kappa}) = \{\mathbf{x} \in \mathcal{X} \mid \exists s, \mathbf{r} : (21a)-(21d)\}. \quad (22)$$

In the following section, we analyze the properties of $\mathcal{X}_{SFLA}(\boldsymbol{\kappa})$ under various choices of $\boldsymbol{\kappa}$.

3.2. Theoretical Properties and Analysis

This section demonstrates that the proposed SFLA set, $\mathcal{X}_{SFLA}(\boldsymbol{\kappa})$, forms an inner-approximation to \mathcal{X}_{Exact} and can offer a less-conservative alternative to the LA set $\mathcal{X}_{LA}(\boldsymbol{\kappa})$. All the corresponding proofs can be found in Appendix B.

We first show that the proposed SFLA achieves an inner-approximation to RHS-WDRJCC:

THEOREM 1. $\mathcal{X}_{SFLA}(\boldsymbol{\kappa})$ is a subset of \mathcal{X}_{Exact} , i.e., $\mathcal{X}_{SFLA}(\boldsymbol{\kappa}) \subseteq \mathcal{X}_{Exact}$.

Observing Eq. (21c) in SFLA $\mathcal{X}_{SFLA}(\boldsymbol{\kappa})$, we can see that only $\lfloor \epsilon N \rfloor P$ constraints are replaced with the conservative approximated distance function $\widehat{\text{dist}}(\boldsymbol{\xi}_i, \mathcal{S}(\mathbf{x}))$. This selective replacement is central to making $\mathcal{X}_{SFLA}(\boldsymbol{\kappa})$ potentially less conservative than $\mathcal{X}_{LA}(\boldsymbol{\kappa})$. To further investigate this, we start with demonstrating that $\mathcal{X}_{LA}(\boldsymbol{\kappa})$ admits a CVaR interpretation:

LEMMA 2. $\mathcal{X}_{LA}(\boldsymbol{\kappa})$ in (16) is equivalent to the following set:

$$\left\{ \mathbf{x} \in \mathcal{X} : \theta/\epsilon + \mathbb{P}_N\text{-CVaR}_{1-\epsilon}(-\widehat{\text{dist}}(\boldsymbol{\xi}, \mathcal{S}(\mathbf{x}))) \leq 0 \right\}, \quad (23)$$

where

$$\mathbb{P}_N\text{-CVaR}_{1-\epsilon}(v(\boldsymbol{\xi})) := \min_{s'} \left\{ s' + \frac{1}{\epsilon N} \sum_{i \in [N]} \max\{0, v(\boldsymbol{\xi}_i) - s'\} \right\} \quad (24)$$

is the CVaR of the random variable $v(\boldsymbol{\xi})$ under the empirical probability distribution constructed by historical data \mathbb{P}_N (Prékopa 2013).

Based on Lemma 2, we can conclude an extended version of Lemma 1 for the approximated distance function $\widehat{\text{dist}}(\cdot)$:

LEMMA 3. For any $\mathbf{x} \in \mathcal{X}_{LA}(\boldsymbol{\kappa})$, there exists (\mathbf{r}, s) such that s is equal to the $(k+1)$ -th smallest value amongst $\{\widehat{\text{dist}}(\boldsymbol{\xi}_i, \mathcal{S}(\mathbf{x}))\}_{i \in [N]}$ and the constraints in (16), namely (15a)–(15c), are satisfied.

With all results above, we now show that the proposed SFLA $\mathcal{X}_{SFLA}(\boldsymbol{\kappa})$ is a less conservative (or at least equally conservative) approximation compared to the LA set $\mathcal{X}_{LA}(\boldsymbol{\kappa})$.

THEOREM 2. The SFLA set $\mathcal{X}_{SFLA}(\boldsymbol{\kappa})$ is a superset of $\mathcal{X}_{LA}(\boldsymbol{\kappa})$, i.e., $\mathcal{X}_{LA}(\boldsymbol{\kappa}) \subseteq \mathcal{X}_{SFLA}(\boldsymbol{\kappa})$.

Theorems 1 and 2 establish that the SFLA set achieves an approximation less conservative than LA and is an inner-approximation to RHS-WDRJCC as well, i.e., $\mathcal{X}_{\text{Exact}} \supseteq \mathcal{X}_{SFLA}(\boldsymbol{\kappa}) \supseteq \mathcal{X}_{LA}(\boldsymbol{\kappa})$. Moreover, all properties of $\mathcal{X}_{LA}(\boldsymbol{\kappa})$ demonstrated by Chen et al. (2023) naturally extend to our proposed $\mathcal{X}_{SFLA}(\boldsymbol{\kappa})$. For example, Chen et al. (2023) showed (Proposition 8) that the good approximation quality of $\mathcal{X}_{LA}(\boldsymbol{\kappa})$ is supported by the fact that its constraints (15a)–(15c) define the best set of inner convex approximations in the $(\mathbf{x}, s, \mathbf{r})$ -feasible region of the exact RHS-WDRJCC reformulation defined by (7). Therefore, the good approximation quality also holds for the proposed SFLA given Theorem 2.

In addition, we show that the SFLA can be exact by integrating $\boldsymbol{\kappa}$ as extra decision variables:

COROLLARY 1. Let $\boldsymbol{\kappa} \in [0, 1]^N$ be extra decision variables and define the updated SFLA set as:

$$\mathcal{X}_{SFLA}^* = \left\{ \mathbf{x} \in \mathcal{X} \mid \exists \boldsymbol{\kappa} \in [0, 1]^N, s, \mathbf{r} : (21a)\text{--}(21d) \right\}.$$

Then we have $\mathcal{X}_{SFLA}^* = \mathcal{X}_{\text{Exact}}$.

Taking $\boldsymbol{\kappa} = \{\kappa_i\}_{i \in [N]}$ as extra decision variab renders the problem bilinear and thus difficult to solve. However, if we restrict $\boldsymbol{\kappa}$ to be uniform, namely $\kappa_i = \kappa$ or equivalently $\boldsymbol{\kappa} = \kappa \mathbf{1}$ (recall that $\kappa_i \in [0, 1]$), then $\boldsymbol{\kappa} = \mathbf{1}$ is the optimal parameter setting:

COROLLARY 2. $\mathcal{X}_{SFLA}(\mathbf{1}) \supseteq \mathcal{X}_{SFLA}(\kappa \mathbf{1})$ for $\forall \kappa \in [0, 1]$.

The proof is similar to that for Proposition 10 in Chen et al. (2023). In fact, for $\boldsymbol{\kappa} = \mathbf{1}$, our proposed SFLA becomes equivalent to the approximation proposed by Chen et al. (2023):

COROLLARY 3. $\mathcal{X}_{SFLA}(\mathbf{1}) = \mathcal{X}_{LA}(\mathbf{1})$.

Note that, for $\boldsymbol{\kappa} \neq \mathbf{1}$, it is possible that the proposed $\mathcal{X}_{SFLA}(\boldsymbol{\kappa})$ strictly dominates $\mathcal{X}_{LA}(\boldsymbol{\kappa})$, namely $\mathcal{X}_{SFLA}(\boldsymbol{\kappa}) \supset \mathcal{X}_{LA}(\boldsymbol{\kappa})$. We have numerically validated this argument by comparing $\mathcal{X}_{SFLA}(\boldsymbol{\kappa})$ and $\mathcal{X}_{LA}(\boldsymbol{\kappa})$ under randomly generated $\boldsymbol{\kappa}$ subject to $\boldsymbol{\kappa} \neq \mathbf{1}$.

In addition, the proposed SFLA $\mathcal{X}_{SFLA}(\boldsymbol{\kappa})$ becomes equivalent to W-CVaR in (12) with a specific setting of \boldsymbol{w} and $\boldsymbol{\kappa} = \mathbf{1}$:

COROLLARY 4. $\mathcal{X}_{SFLA}(\mathbf{1}) = \mathcal{X}_{WCVaR}(\boldsymbol{w}^*)$, where $\boldsymbol{w}^* = [w_p^*]_{p \in [P]}$ and $w_p^* = \frac{\|\boldsymbol{b}_p\|_*^{-1}}{\sum_{l \in [P]} \|\boldsymbol{b}_l\|_*^{-1}}$.

Finally, there are conditions when the proposed SFLA $\mathcal{X}_{SFLA}(\mathbf{1})$ becomes exact for $\boldsymbol{\kappa} = \mathbf{1}$:

COROLLARY 5. $\mathcal{X}_{SFLA}(\mathbf{1}) = \mathcal{X}_{Exact}$ holds for either the following conditions:

- (1) We have $\boldsymbol{\xi}_i \in \mathcal{S}(\boldsymbol{x})$ for all $i \in [N]$ and $\boldsymbol{x} \in \mathcal{X}_{Exact}$.
- (2) We have $\epsilon \leq 1/N$.

The second condition in Corollary 5 shows that the proposed SFLA becomes exact when the number of data N is small or the risk level ϵ is low. This also implies that a smaller N and a smaller ϵ can lead to better approximation quality of the proposed SFLA. This implication is particularly important, as DRCCP is often used in cases with limited historical data due to its strong out-of-sample performance. Additionally, safety-critical applications, such as in power systems, generally demand a low risk level. Thus, the proposed SFLA can achieve high approximation quality across a range of practical applications.

Finally, as demonstrated by Chen et al. (2022), a larger Wasserstein radius θ would convexify \mathcal{X}_{Exact} , which also suggests an increasing approximation quality of the proposed SFLA $\mathcal{X}_{SFLA}(\boldsymbol{\kappa})$ with the increase of θ .

4. Numerical Experiments

This section presents numerical case studies to demonstrate the reduction of computational complexity and also the approximation quality of the proposed SFLA. Specifically, Section 4.1 investigates a single-level UC problem and Section 4.2 explores a bilevel storage strategic bidding problem. For all norm calculations in the RHS-WDRJCC formulations, we adopt the L2 norm which has the property of being self-dual.

Both of the numerical cases are programmed by Python 3.9.19 and solved by Gurobi 11.0.3 on a server with dual AMD EPYC 7532 CPUs and 256 GB RAM. The solver is configured as `FeasibilityTol=1e-9`, `OptimalityTol=1e-9`, `IntFeasTol=1e-9`, `MIPGap=0.1%`, `Threads=4`, and a one-hour wall-clock time limit `TimeLimit=3600s`; other solver parameters are set to default values. We examine two risk levels $\epsilon \in \{0.025, 0.05\}$. For the Wasserstein radius θ , we evaluate a small value that leads to a slightly less reliable result (the out-of-sample JCC satisfaction rate being lower than desired) and a large value that includes a slightly conservative result. We set $\kappa = \mathbf{1}$ for the proposed SFLA and LA, $w_p = 1/P$ for W-CVaR following Ordoudis et al. (2021), and $\epsilon_p = \epsilon/P$ for Bonferroni approximation. Detailed case study settings for the UC and bilevel problems, including datasets and the generation of random runs to ensure robust conclusions, are given in Appendices C.1 and D.1. The code alongside the mathematical formulations for our UC and bilevel problems are available at our GitHub repository <https://github.com/PSALOxford/SFLA>.

4.1. Unit Commitment Problem

The first case study examines a chance-constrained UC problem. UC represents a typical real-world large-scale problem, and its primary objective is to determine the generator on/off statuses for the next scheduling period with a minimal operation cost (Chen et al. 2016). UC is typically formulated as an MIP, where each generator requires at least T binary variables to represent on/off statuses over the next T time steps. With thousands of generators (e.g., 1400 in MISO), non-linear generator cost functions (Xu et al. 2017), and complex network constraints, UC is challenging to solve even in a deterministic case. However, the integration of renewables introduces additional uncertainty into UC, making chance constraints essential to ensure reliability (Wang et al. 2016, Wu et al. 2016, Yang et al. 2020). Given UC’s inherent complexity, minimizing the added computational burden of JCCs is critical.

We compare the proposed SFLA with benchmarks including ExactS (Ho-Nguyen et al. 2021) in Eq. (25), LA (Chen et al. 2023) in Eq. (16), W-CVaR (Mohajerin Esfahani and Kuhn 2018, Chen et al. 2023) in Eq. (13), and Bonferroni approximation (Chen et al. 2023) in Eq. (10). Details of the UC formulation are provided in our GitHub repository.

4.1.1. Evaluation Metrics The UC problem is primarily evaluated using the following metrics:

1. *TimeF* (s): This metric records the time (in seconds) to obtain the first “comparable high-quality” solution, defined as the solution with an objective within the `MIPGap` of the final objective achieved by the proposed SFLA (whether optimal or the best found within the `TimeLimit`). If SFLA does not yield a feasible solution within the `TimeLimit`, the *TimeF* of the proposed SFLA is set to the `TimeLimit`, and the *TimeF* for other benchmarks is set to the time when the first feasible solution is found (if any, otherwise set to the `TimeLimit`). Because MIP admits early stop, this metric offers a practical perspective in cases where the solver identifies a solution close to optimal early but requires extra time for verifying optimality.
2. *Time* (s): This measures the total time (in seconds) spent to solve the problem to optimality (within `MIPGap`), and is set to the `TimeLimit` if no optimal solution is found within the `TimeLimit`. This metric compliments the previous *TimeF* by providing verified optimality.
3. *Obj. Diff.* (%): This is the percentage difference between the optimal value (minimum UC cost) of a benchmark method and that of the SFLA, relative to the optimal value of the SFLA. A positive value indicates that the benchmark achieves a lower cost (better optimality) than the SFLA. We only keep certain random runs where the benchmark method and the proposed SFLA are both solved to optimality.
4. *Reli.* (%): This is the out-of-sample joint satisfaction rate of the RHS-WDRJCC. This metric is used to justify the reasonability of the selection of Wasserstein radius θ , and is calculated on 5000 held-out samples.

This section prioritizes *TimeF* over the total computation time *Time* due to comparison with ExactS. MIP can always have early-stopping and ExactS can have better optimality compared to inner-approximations (SFLA, LA, W-CVaR and Bonferroni). Therefore, a higher *Time* for ExactS does not necessarily suggest its disadvantage.

4.1.2. Results for Unit Commitment Our main content specifically focuses on the comparison between the proposed SFLA and ExactS. Comparisons with LA, W-CVaR, and Bonferroni are excluded here due to their significant disadvantages relative to the proposed SFLA as demonstrated in Appendix C.2. Also, our numerical results suggest that both the proposed SFLA and ExactS exhibit variability. To reach a more robust conclusion, we test a range of parameter settings and implement 150 random runs for each setting. Figure 3 visualizes the distribution of the *TimeF* metric, while the mean values and the computational speedup of the proposed SFLA over ExactS are summarized in Table 1. As can be seen, except for a single parameter setting ($\epsilon = 0.025, \theta =$

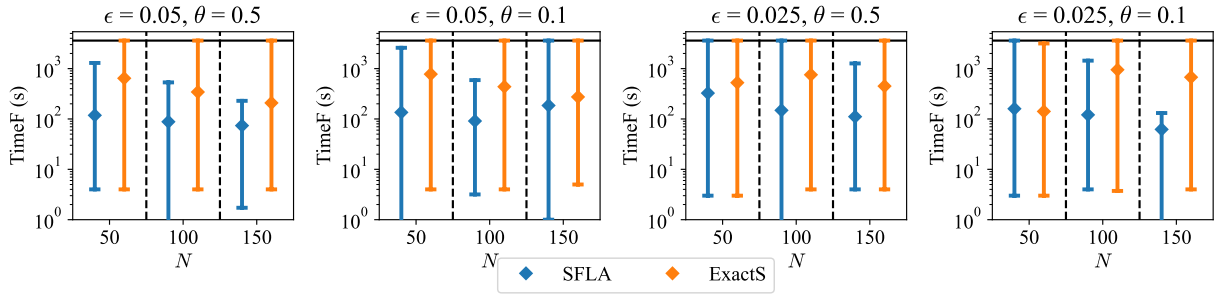


Figure 3 Computation time to obtain the first comparable high-quality solution for the proposed SFLA and the benchmark ExactS for the UC problem.

Note. Dots represent the mean value of the 150 random runs, with error bars indicating the 95% percentile interval (from 2.5th to 97.5th). The black horizontal line represents the 3600s TimeLimit. The optimization horizon is set to $T = 24$.

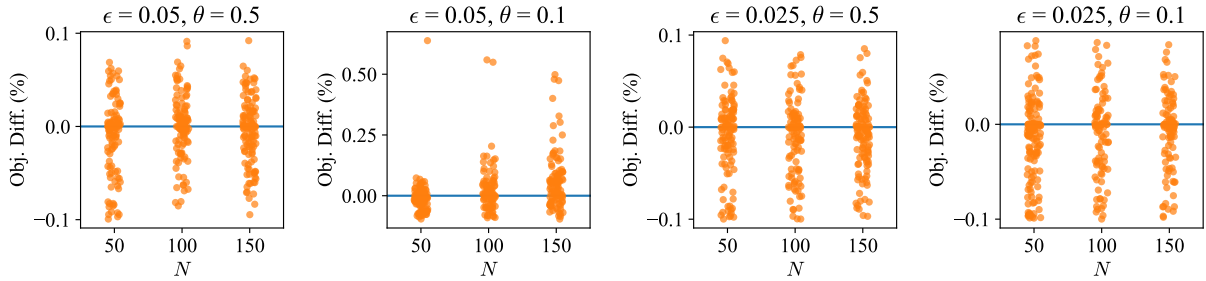


Figure 4 Performance comparison of the optimality for the proposed SFLA and the benchmark ExactS for the UC problem.

Note. Each round dot represents a result of one of the 150 random runs. The blue horizontal line indicates a zero difference of the optimal value of a benchmark method compared to the proposed SFLA. Values higher than this horizontal line indicate that the benchmark achieves lower cost (better optimality) than the proposed SFLA. The optimization horizon is set to $T = 24$.

Table 1 Performance comparison of the final solution for the UC problem

ϵ	θ	N	<i>TimeF</i> (s)		<i>Time</i> (s)		<i>Reli.</i> (%)		<i>Obj. Diff.</i> (%)
			SFLA	ExactS	SFLA	ExactS	SFLA	ExactS	
0.05	0.5	50	118.17	643.19 (5.44 \times)	376.25	812.62 (2.16 \times)	99.14	99.20	-0.010
		100	88.04	343.21 (3.90 \times)	512.4	473.42 (0.92 \times)	99.67	99.68	0.001
		150	73.82	208.25 (2.82 \times)	471.25	288.92 (0.61 \times)	99.80	99.80	-0.004
	0.1	50	135.24	776.37 (5.74 \times)	576.6	1098.01 (1.90 \times)	76.01	76.88	-0.008
		100	91.07	437.21 (4.80 \times)	521.25	1064.36 (2.04 \times)	88.03	88.51	0.027
		150	185.28	273.93 (1.48 \times)	451.55	834.81 (1.85 \times)	91.87	92.14	0.061
0.025	0.5	50	326.1	525.47 (1.61 \times)	353.36	529.32 (1.50 \times)	100.00	100.00	-0.008
		100	148.47	754.92 (5.08 \times)	459.6	827.44 (1.80 \times)	100.00	100.00	-0.011
		150	111.05	449.19 (4.04 \times)	331.49	636.40 (1.92 \times)	100.00	100.00	-0.010
	0.1	50	159.67	141.29 (0.88 \times)	186.68	173.72 (0.93 \times)	87.81	87.75	-0.015
		100	120.77	949.39 (7.86 \times)	531.27	1079.66 (2.03 \times)	94.44	94.78	-0.009
		150	62.11	674.81 (10.86 \times)	605.29	1100.77 (1.82 \times)	96.45	96.71	-0.008

Each entry represents the mean value over 150 random runs. In columns *TimeF* (s) and *Time* (s), values in parenthesis represent the speed-up rate, i.e., the ratio of the time metrics of ExactS relative to the proposed SFLA.

0.1, $N = 50$) where the proposed SFLA shows a minor underperformance (12% slower), the SFLA demonstrates significant computational speedup in *TimeF* over ExactS: the computational speedup reaches 10× for a parameter setting ($\epsilon = 0.025$, $\theta = 0.1$, $N = 150$), and the speedup is 3.8× for the average *TimeF* of the 12 parameter settings. Moreover, as shown in Figure 3, the upper bounds of the error bars (97.5-th percentile) for the proposed SFLA are lower than those of ExactS in 8 out of 12 parameter settings and comparable in the remaining settings, indicating a reduced likelihood of extreme cases with prolonged computation times.

Regarding the time required to achieve optimality (*Time*), Table 1 shows that the proposed SFLA demonstrates slower performance in 3 of 12 settings, indicating challenges in achieving the final minor solution improvements needed to meet the desired MIPGap. However, the speedup rate is still around 1.7× for the average *Time* of the 12 parameter settings, suggesting an overall advantage of the proposed SFLA over ExactS.

Figure 4 compares the quality of the optimal solution of the proposed SFLA with that of ExactS. In most random runs and most parameter settings, the *Obj. Diff.* is within the preset MIPGap, demonstrating comparable optimal solution quality between the proposed SFLA and ExactS. Slight underperformance (less than 0.6%) for certain random runs appears only under the combination of a high risk ($\epsilon = 0.05$), a small radius ($\theta = 0.1$), and a large number of samples ($N \geq 100$), which is consistent with Corollary 5 and the related discussions. However, among these underperformed parameter settings, the average underperformance is still below 0.061% as presented in Table 1. In addition, real-world applications such as those found in power systems have a small tolerance for risk, making the proposed SFLA an effective approximation method.

Our Appendix C.2 further compares the proposed SFLA and ExactS in different problem scales (different T). It is observed that the proposed SFLA preserves computational efficiency in more complex cases without sacrificing optimality, making it particularly advantageous for practical high-complexity applications such as UC.

4.2. Bilevel Storage Strategic Bidding Problem

This section explores a bilevel optimization problem that allows a price-maker energy storage operator to maximize its profit by participating in a joint day-ahead energy and reserve market. The market participation process can be summarized as follows: Participants submit their bids and offers for each energy and reserve product for specific future delivery times. Bids represent the provision of services to the power system, such as generating power or supplying reserve capacity, while offers involve procuring services, such as purchasing energy for storage charging. In line with most

established power markets, we model each bid or offer as a price-quantity pair that is submitted to the market for clearing, which then determines a market clearing price (marginal price) and cleared quantities bounded by the submitted bid-offer quantities. Upon settlement, market participants receive payment or incur charges at the market clearing price for their respective cleared quantities, with a binding obligation to fulfill these quantities.

An energy storage operator transitions from a price-taker to a price-maker when its storage power capacity is large enough to influence market outcomes. To maximize profit, the storage operator determines the optimal bidding or offering strategy by solving a bilevel strategic bidding problem, where the lower level models the market clearing process (Nasrolahpour et al. 2018, Tómasson et al. 2020, Dimitriadis et al. 2022, Wang et al. 2017). With increasing uncertainty due to renewable generation, the market clearing process can incorporate chance constraints (RHS-WDRJCC), such as those in the UC problem (see Section 4.1). Therefore, to accurately model the market clearing process, the bilevel problem needs to incorporate a RHS-WDRJCC in the lower level. Consequently, convex approximations to RHS-WDRJCC become important for transforming the bilevel problem into a solvable single-level counterpart via KKT conditions or strong duality conditions. Note that chance constraints at lower levels frequently arise in bilevel and multilevel optimization problems, where uncertainty is revealed after lower-level decisions (Beck et al. 2023). Another example is the European multilevel gas market clearing problem studied by Heitsch et al. (2022).

This section compares the proposed SFLA with typical convex approximation benchmarks including LA (Chen et al. 2023) in Eq. (16), W-CVaR (Mohajerin Esfahani and Kuhn 2018, Chen et al. 2023) in Eq. (13), and Bonferroni approximation (Chen et al. 2023) in Eq. (10). For all the RHS-WDRJCC approximations, the corresponding bilevel problems are reformulated as single-level mixed-integer nonlinear non-convex programming problems, where the lower-level problem is replaced by the corresponding KKT optimality conditions, which can be solved using the Gurobi solver. ExactS is not included because bilevel problem solving requires convexity at the lower level. The bilevel formulation and also the corresponding single-level reformulation using KKT can be found in our online GitHub repository.

4.2.1. Evaluation Metrics The exclusive evaluation metrics used in this case study include:

1. *N Infeasible*: This is the number of random runs that are infeasible. We introduce this metric because the high complexity of the bilevel problem introduces numerical issues that may make solvers incorrectly assess a feasible instance as infeasible. In our case studies, this happens in certain runs where LA and W-CVaR are incorrectly assessed as infeasible, but the feasibility

can be recovered by setting `NumericalFocus=3`, which increases numerical stability at the cost of longer the solving time. A large value of this metric indicates that the method is prone to numerical issues, especially for LA and W-CVaR.

2. *Bilevel Profit* (k\$): This represents the optimal profit of storage systems, which is the objective obtained by solving the bilevel problem.
3. *Actual Profit* (k\$): The market clearing process is modeled as a single-level problem, where the market operator uses the exact MIP reformulation of RHS-WDRJCC to maximize social welfare, consistent with the ExactS approach in Section 4.1. Therefore, the use of ExactS may cause *Bilevel Profit* to differ from *Actual Profit*. We calculate *Actual Profit* through the following steps: 1) Retrieve the bids and offers from the bilevel problem solutions; 2) Adjust bid prices slightly downward and offer prices slightly upward (by $\$10^{-5}$), setting bid quantities to zero when the bilevel-cleared quantities are zero—these adjustments ensure the desired acceptance or rejection behaviors modeled in the bilevel problem; 3) Input these modified bids and offers into the actual market clearing problem with ExactS (MIP); 4) Calculate the actual market clearing price, which is then used to compute the *Actual Profit* of the storage operator. Due to the MIP formulation in ExactS, optimal dual variables cannot be directly used to determine marginal prices. Instead, we use sensitivity analysis to calculate the clearing price, by comparing the change of the objective function of the actual market clearing after a 10^{-3} MW increase in demand for each time step.
4. *Actual Profit Diff* (k\$): The difference of *Actual Profit* between a benchmark method and that calculated by the proposed SFLA. A negative value represents a lower profit compared to SFLA. We do not use the percentage difference as is in our UC case because the profit could be close to zero, leading to exacerbated results. When calculating *Actual Profit Diff*, we consider only those random runs where both the proposed SFLA and the benchmark identify feasible solutions within the prescribed `TimeLimit`.

4.2.2. Results for Bilevel Strategic Bidding Figure 5 visualizes the distributions of the evaluation metrics for the proposed SFLA and three benchmarks, i.e., LA, W-CVaR, and Bonferroni. As can be observed from the first two columns of Figure 5, the proposed SFLA demonstrates significant speedup in both *Time* and *TimeF*; to facilitate interpretation, Table 2 in Appendix D lists the mean values of these time metrics along with the corresponding speedup rates. In particular, the proposed SFLA achieves a speedup of up to 90× in solving to optimality (*Time*) compared to LA and W-CVaR, and the speedup is up to 40× in finding the first comparable high-quality solution (*TimeF*)

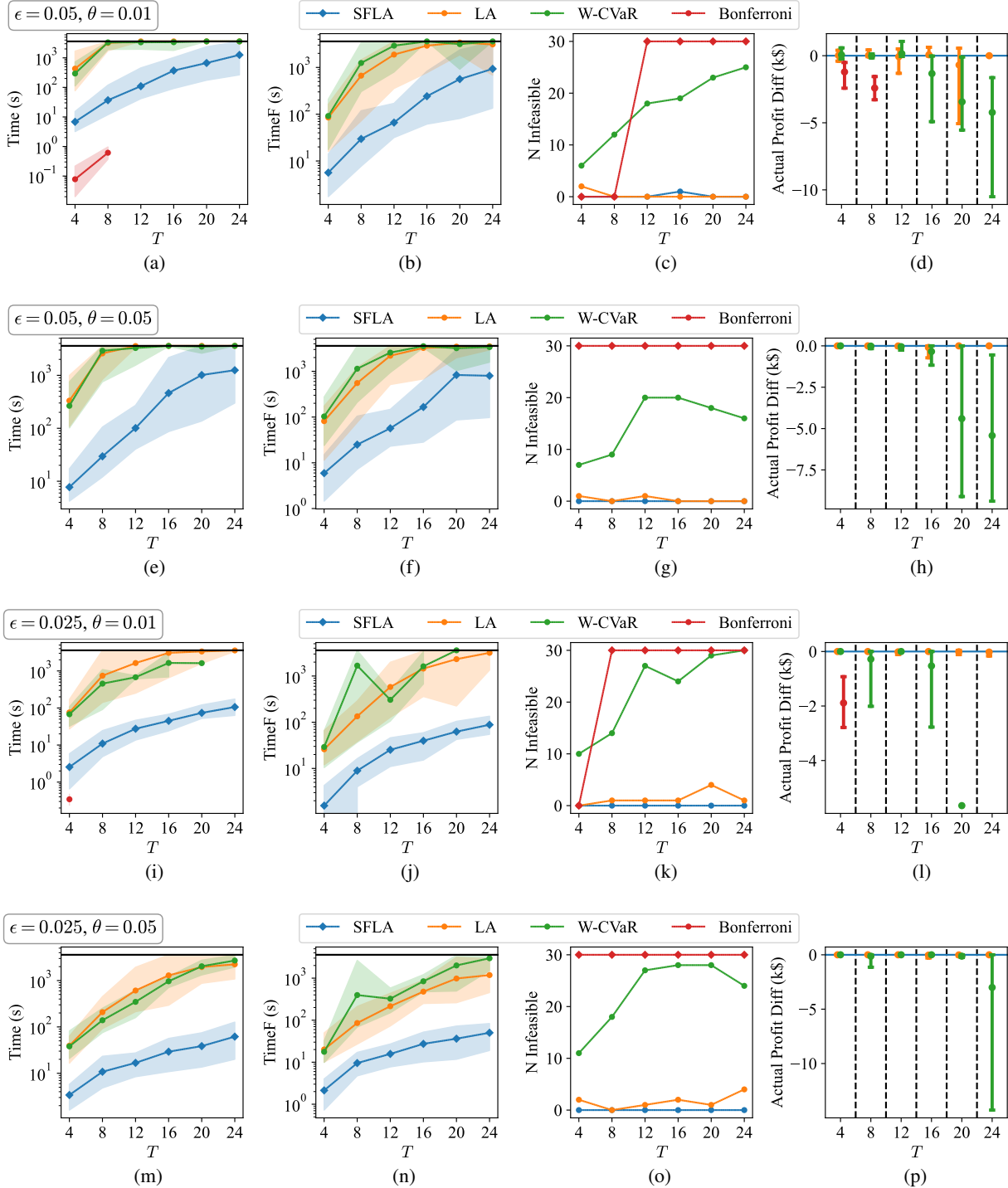


Figure 5 Performance comparison for the bilevel problem.

Note. The evaluations are based on different parameter combinations of risk level (ϵ), radius (θ) parameters, and the number of time steps T . Subplots (e)–(p) replicate (a)–(d) but for varying (ϵ, θ) combinations. The black horizontal line represents the 3600s TimeLimit. Dots represent the mean values of the 30 random runs, with shaded areas representing the 95% percentile interval (from 2.5th to 97.5th). The blue horizontal line indicates a zero difference of the optimal value compared to the proposed SFLA. The TimeF (s) of Bonferroni approximation is not displayed because Bonferroni approximation is overly conservative such that it can easily find high *Bilevel Profit* (k\$) (the bilevel objective value) but poor *Actual Profit* (k\$) (plots 5d and 5l).

relative to LA and $180\times$ relative to W-CVaR. Although the Bonferroni approximation achieves the fastest computation, its over-conservativeness leads to infeasibility in the majority of parameter settings. It should be noted that the speedup rates compared to LA and W-CVaR decrease for a large T especially for $\epsilon = 0.05$; this is because LA and W-CVaR reach the `TimeLimit` rather than due to a reduction in the computational superiority of the proposed SFLA.

Furthermore, as can be observed in the third column of Figure 5, W-CVaR shows a large number of infeasible runs. These infeasibilities are resolved by setting `NumericalFocus=3`, indicating numerical issues. While LA is more numerically stable, it still incurs 22 infeasible runs in total. In contrast, the proposed SFLA has only one infeasible run, demonstrating its higher numerical stability. Note that the infeasibility of the Bonferroni approximation is caused by its over-conservativeness that cannot be recovered by setting `NumericalFocus=3`.

The fourth column of Figure 5 compares the *Actual Profit* of the benchmarks with that of the proposed SFLA. Among the feasible cases, Bonferroni approximation leads to significantly lower profit than other methods because of its over-conservativeness. It is noteworthy that both LA and W-CVaR can occasionally yield either higher or lower profits than the proposed SFLA. This variability arises because the market clearing modeled in the bilevel problem does not precisely replicate the actual market clearing process (cleared with exact MIP-based RHS-WDRJCC), and bilevel problems admit multiple solutions even at optimality. Thus, even when different methods yield the same *Bilevel Profit*, discrepancies can still arise in *Actual Profit*. It should be noted that W-CVaR shows significantly lower *Actual Profit* especially for a large T , because W-CVaR fails to find a good feasible solution within the `TimeLimit`, rather than due to over-conservativeness.

5. Conclusion

This work proposes a novel Strengthened and Faster Linear Approximation (SFLA) for Wasserstein distributionally robust joint chance constraints under right-hand-side uncertainty (RHS-WDRJCC). The proposed SFLA enables more efficient and less conservative solutions to a class of real-world large-scale chance-constrained optimization problems, such as chance-constrained unit commitment (UC) and bilevel optimization for strategic bidding in electricity markets with chance-constrained economic dispatch. By applying valid inequalities to an existing linear approximation (LA) that is equivalent to the worst-case conditional value-at-risk (W-CVaR) method under specific hyperparameters, the proposed SFLA reduces the number of constraints and tightens the feasible region for the ancillary variables, resulting in a significant computational speedup. Despite this

tightening, we prove that the proposed SFLA does not introduce additional conservativeness and can even be a less conservative inner-approximation compared to LA. Furthermore, we provide guidance in setting the hyperparameters of the proposed SFLA, which corresponds to the least conservativeness when hyperparameters are restricted to be uniform. We also analyze conditions under which the proposed SFLA is equivalent to LA and W-CVaR.

Extensive numerical experiments demonstrate the superiority and significance of the proposed SFLA. In the UC problem, we demonstrate that the proposed SFLA achieves up to $10\times$ and on average $3.8\times$ computational speedup compared to the existing exact and strengthened MIP reformulation (ExactS) in finding comparable high-quality solutions. We also demonstrate that the proposed SFLA achieves approximation quality comparable to the exact reformulation ExactS, except for minor inferiority only under the combination of a high risk ϵ , a large number of historical data (N), and a small ambiguity set radius θ . In the bilevel strategic bidding problem where the exact formulation is not applicable due to its non-convexity, the proposed SFLA can lead to $90\times$ computational speedup than existing linear approximation methods (LA and W-CVaR).

It is worth noting that the applications of the proposed SFLA are not limited to the UC and bilevel energy bidding problems demonstrated in this paper. The method is also applicable to other large-scale, real-world problems that are already complex in their deterministic form and require tractable approaches to handle uncertainty. Examples include large-scale transportation problems, multilevel market clearing problems, and multilevel infrastructure planning that includes a lower-level market cleared before uncertainty realization.

Historical data plays a significant role that affects the complexity and solution quality of WDR-JCC, including the proposed SFLA. Future work could also explore scenario reduction techniques (Arpón et al. 2018) to further improve the performance of the proposed SFLA.

Acknowledgments

This paper was supported by the Engineering and Physical Sciences Research Council (EPSRC) (grant reference number EP/W027321/1). Yihong Zhou's and Yuxin Xia's work were also supported by the Engineering Studentship from the University of Edinburgh.

References

- Arpón S, Homem-de Mello T, Pagnoncelli B (2018) Scenario reduction for stochastic programs with conditional value-at-risk. *Mathematical Programming* 170(1):327–356.
- Beck Y, Ljubić I, Schmidt M (2023) A survey on bilevel optimization under uncertainty. *European Journal of Operational Research* 311(2):401–426.

- Chen X, Sim M, Sun P (2007) A robust optimization perspective on stochastic programming. *Operations research* 55(6):1058–1071.
- Chen Y, Casto A, Wang F, Wang Q, Wang X, Wan J (2016) Improving large scale day-ahead security constrained unit commitment performance. *IEEE Transactions on Power Systems* 31(6):4732–4743.
- Chen Z, Kuhn D, Wiesemann W (2022) Data-driven chance constrained programs over wasserstein balls. *Operations Research* .
- Chen Z, Kuhn D, Wiesemann W (2023) On approximations of data-driven chance constrained programs over wasserstein balls. *Operations Research Letters* 51(3):226–233.
- Delage E, Ye Y (2010) Distributionally robust optimization under moment uncertainty with application to data-driven problems. *Operations research* 58(3):595–612.
- Dimitriadis CN, Tsimopoulos EG, Georgiadis MC (2022) Strategic bidding of an energy storage agent in a joint energy and reserve market under stochastic generation. *Energy* 242:123026, ISSN 0360-5442.
- Ding Y, Morstyn T, McCulloch MD (2022) Distributionally robust joint chance-constrained optimization for networked microgrids considering contingencies and renewable uncertainty. *IEEE Trans. on Smart Grid* 13(3):2467–2478.
- Gabrel V, Murat C, Thiele A (2014) Recent advances in robust optimization: An overview. *European journal of operational research* 235(3):471–483.
- Gao R, Kleywegt A (2023) Distributionally robust stochastic optimization with wasserstein distance. *Mathematics of Operations Research* 48(2):603–655.
- Geng X, Xie L (2019) Data-driven decision making in power systems with probabilistic guarantees: Theory and applications of chance-constrained optimization. *Annual reviews in control* 47.
- Gurobi Optimization, LLC (2024) Gurobi Optimizer Reference Manual. URL <https://www.gurobi.com>.
- Heitsch H, Henrion R, Kleinert T, Schmidt M (2022) On convex lower-level black-box constraints in bilevel optimization with an application to gas market models with chance constraints. *Journal of Global Optimization* 84(3):651–685.
- Ho-Nguyen N, Kılınç-Karzan F, Küçükyavuz S, Lee D (2021) Distributionally robust chance-constrained programs with right-hand side uncertainty under wasserstein ambiguity. *Mathematical Programming* .
- Hong T, Glider, Pinson P (2012) Global Energy Forecasting Competition 2012 - Wind Forecasting. <https://kaggle.com/competitions/GEF2012-wind-forecasting>, accessed: 2024-10-11.
- Hong T, Pinson P, Fan S (2014) Global energy forecasting competition 2012.
- Illinois Center for a Smarter Electric Grid (ICSEG) (1979) IEEE 24-bus system. <https://icseg.iti.illinois.edu/ieee-24-bus-system/>, accessed: 2024-10-11.
- Jiang N, Xie W (2022) ALSO-X and ALSO-X+: Better convex approximations for chance constrained programs. *Operations Research* 70(6):3581–3600.
- Jiang N, Xie W (2024a) ALSO-X#: Better convex approximations for distributionally robust chance constrained programs. *Mathematical Programming* 1–64.

-
- Jiang N, Xie W (2024b) The terminator: An integration of inner and outer approximations for solving wasserstein distributionally robust chance constrained programs via variable fixing. *INFORMS Journal on Computing* .
- Mohajerin Esfahani P, Kuhn D (2018) Data-driven distributionally robust optimization using the wasserstein metric: Performance guarantees and tractable reformulations. *Mathematical Programming* 171(1):115–166.
- Nasrolahpour E, Kazempour J, Zareipour H, Rosehart WD (2018) A bilevel model for participation of a storage system in energy and reserve markets. *IEEE Transactions on Sustainable Energy* 9(2):582–598.
- Ordoudis C, Nguyen VA, Kuhn D, Pinson P (2021) Energy and reserve dispatch with distributionally robust joint chance constraints. *Operations Research Letters* 49(3):291–299.
- Paredes Á, Aguado JA, Essayeh C, Xia Y, Savelli I, Morstyn T (2023) Stacking revenues from flexible ders in multi-scale markets using tri-level optimization. *IEEE Transactions on Power Systems* 39(2):3949–3961.
- Prékopa A (2013) *Stochastic programming*, volume 324 (Springer Science & Business Media).
- Scarf HE, Arrow K, Karlin S (1957) *A min-max solution of an inventory problem* (Rand Corporation Santa Monica).
- Sun X, Luh PB, Bragin MA, Chen Y, Wan J, Wang F (2018) A novel decomposition and coordination approach for large day-ahead unit commitment with combined cycle units. *IEEE Transactions on Power Systems* 33(5):5297–5308.
- Tómasson E, Hesamzadeh MR, Wolak FA (2020) Optimal offer-bid strategy of an energy storage portfolio: A linear quasi-relaxation approach. *Applied Energy* 260:114251, ISSN 0306-2619.
- van Ackooij W, Finardi EC, Ramalho GM (2018) An exact solution method for the hydrothermal unit commitment under wind power uncertainty with joint probability constraints. *IEEE Transactions on Power Systems* 33(6):6487–6500.
- Wang Y, Dvorkin Y, Fernández-Blanco R, Xu B, Qiu T, Kirschen DS (2017) Look-ahead bidding strategy for energy storage. *IEEE Transactions on Sustainable Energy* 8(3):1106–1117.
- Wang Y, Zhao S, Zhou Z, Botterud A, Xu Y, Chen R (2016) Risk adjustable day-ahead unit commitment with wind power based on chance constrained goal programming. *IEEE Transactions on Sustainable Energy* 8(2):530–541.
- Wu Z, Zeng P, Zhang XP, Zhou Q (2016) A solution to the chance-constrained two-stage stochastic program for unit commitment with wind energy integration. *IEEE Transactions on Power Systems* 31(6):4185–4196.
- Xu T, Birchfield AB, Gegner KM, Shetye KS, Overbye TJ (2017) Application of large-scale synthetic power system models for energy economic studies.
- Yang Y, Wu W, Wang B, Li M (2020) Analytical reformulation for stochastic unit commitment considering wind power uncertainty with gaussian mixture model. *IEEE Transactions on Power Systems* 35(4):2769–2782.
- Zhao H, Tanneau M, Hentenryck PV (2024) On the viability of stochastic economic dispatch for real-time energy market clearing. URL <https://arxiv.org/abs/2308.06386>.
- Zhou H, Zhou Y, Hu J, Yang G, Xie D, Xue Y, Nordström L (2021) LSTM-based energy management for electric vehicle charging in commercial-building prosumers. *Journal of Modern Power Systems and Clean Energy* 9(5).

Appendix. Supplementary Formulation and Proofs

A. Strengthened and Exact MIP Reformulation

The strengthened exact MIP reformulation (ExactS), presented as Formulation (20) in (Ho-Nguyen et al. 2021), is reproduced below for convenience:

$$\mathbf{z} \in \{0, 1\}^N, s \geq 0, \mathbf{r} \geq \mathbf{0}, \quad (25a)$$

$$\epsilon N s - \sum_{i \in [N]} r_i \geq \theta N, \quad (25b)$$

$$\sum_{i \in [N]} z_i \leq \lfloor \epsilon N \rfloor, \quad (25c)$$

$$M(1 - z_i) \geq s - r_i, \quad \forall i \in [N], \quad (25d)$$

$$\frac{\mathbf{b}_p^\top \boldsymbol{\xi}_i + d_p - \mathbf{a}_p^\top \mathbf{x}}{\|\mathbf{b}_p\|_*} + \frac{-\mathbf{b}_p^\top \boldsymbol{\xi}_i + q_p}{\|\mathbf{b}_p\|_*} z_i \geq s - r_i, \quad \forall i \in [N], p \in [P], \quad (25e)$$

$$\frac{q_p + d_p - \mathbf{a}_p^\top \mathbf{x}}{\|\mathbf{b}_p\|_*} \geq s, \quad \forall p \in [P]. \quad (25f)$$

where all the notations have been defined in the main content. The \mathbf{x} -feasible region of the ExactS can be expressed as:

$$\mathcal{X}_{\text{ExactS}} = \{\mathbf{x} \in \mathcal{X} \mid \exists \mathbf{z}, s, \mathbf{r} : (25a)–(25f)\}. \quad (26)$$

B. Proofs

Proof of Proposition 1

proof Note that the first two constraints in sets (9) and (20) are identical. To show the statement, it suffices to show that replacing the constraint (7c) in set (9) with constraints (19c)–(19d) in set (20) has no impact on the \mathbf{x} -feasible region.

(20) \implies (9): Based on the definition of $[N]_p$, we have:

$$\mathbf{b}_p^\top \boldsymbol{\xi}_i \geq q_p, \quad \forall i \in [N] \setminus [N]_p, p \in [P].$$

Then, based on (19d), for any $i \in [N] \setminus [N]_p$ with $p \in [P]$, we have:

$$\left(\frac{\mathbf{b}_p^\top \boldsymbol{\xi}_i + d_p - \mathbf{a}_p^\top \mathbf{x}}{\|\mathbf{b}_p\|_*} \right)^+ \geq \frac{\mathbf{b}_p^\top \boldsymbol{\xi}_i + d_p - \mathbf{a}_p^\top \mathbf{x}}{\|\mathbf{b}_p\|_*} \geq \frac{q_p + d_p - \mathbf{a}_p^\top \mathbf{x}}{\|\mathbf{b}_p\|_*} \geq s.$$

As $r_i \geq 0$, we further have:

$$\left(\frac{\mathbf{b}_p^\top \boldsymbol{\xi}_i + d_p - \mathbf{a}_p^\top \mathbf{x}}{\|\mathbf{b}_p\|_*} \right)^+ \geq s \geq s - r_i,$$

which, combined with (19c), implies the satisfaction of (7c).

(20) \impliedby (9): Based on Lemma 1, for any $\mathbf{x} \in \mathcal{X}_{\text{Exact}}$ in (9), there always exists (\mathbf{r}^*, s^*) such that s^* is equal to the $(k+1)$ -th smallest value amongst the set $\{\text{dist}(\boldsymbol{\xi}_i, \mathcal{S}(\mathbf{x}))\}_{i \in [N]}$ and constraints (7a)–(7c) are satisfied. Without loss of generality, we assume the following ordering: $\text{dist}(\boldsymbol{\xi}_1, \mathcal{S}(\mathbf{x})) \leq \dots \leq \text{dist}(\boldsymbol{\xi}_N, \mathcal{S}(\mathbf{x}))$. Then denote the $(k+1)$ -th smallest distance value as $\text{dist}^*(\mathbf{x}) := \text{dist}(\boldsymbol{\xi}_{k+1}, \mathcal{S}(\mathbf{x})) = s^*$. Combined with the analytical expression of the distance function in (6), the pair $(\mathbf{x}, \mathbf{r}^*, s^*)$ satisfies the constraints (19a)–(19c). It remains to show the satisfaction of (19d) given the pair $(\mathbf{x}, \mathbf{r}^*, s^*)$.

Now consider two cases:

- If $\text{dist}^*(\mathbf{x}) = 0$, then $s^* = 0$. As (7b) must be satisfied for the given (\mathbf{r}^*, s^*) , this leads to a contradiction because $s^* = 0$ implies the non-positivity of the left-hand side of (7b), but the right-hand side of (7b) is strictly positive due to the assumption $\theta > 0$. Therefore, we must have $\text{dist}^*(\mathbf{x}) > 0$.
- If $\text{dist}^*(\mathbf{x}) > 0$, then for any $p \in [P]$, when $i \geq k + 1$, we have:

$$0 < s^* = \text{dist}^*(\mathbf{x}) \leq \text{dist}(\xi_i, \mathcal{S}(\mathbf{x}))$$

Given $0 < \text{dist}(\xi_i, \mathcal{S}(\mathbf{x}))$, based on (6), we have:

$$\text{dist}(\xi_i, \mathcal{S}(\mathbf{x})) = \min_{p \in [P]} \frac{\mathbf{b}_p^\top \xi_i + d_p - \mathbf{a}_p^\top \mathbf{x}}{\|\mathbf{b}_p\|_*}$$

which leads to:

$$s^* \leq \min_{p \in [P]} \frac{\mathbf{b}_p^\top \xi_i + d_p - \mathbf{a}_p^\top \mathbf{x}}{\|\mathbf{b}_p\|_*} \leq \frac{\mathbf{b}_p^\top \xi_i + d_p - \mathbf{a}_p^\top \mathbf{x}}{\|\mathbf{b}_p\|_*}.$$

In other words, for any $p \in [P]$, there will be at least $N - k$ elements in the set $\left\{ \frac{\mathbf{b}_p^\top \xi_i + d_p - \mathbf{a}_p^\top \mathbf{x}}{\|\mathbf{b}_p\|_*} \right\}_{i \in [N]}$ not smaller than s^* . Since q_p is defined as the $(k + 1)$ -th smallest value of $\{\mathbf{b}_p^\top \xi_i\}_{i \in [N]}$, $\frac{q_p + d_p - \mathbf{a}_p^\top \mathbf{x}}{\|\mathbf{b}_p\|_*}$ is the $(k + 1)$ -th smallest element in the set $\left\{ \frac{\mathbf{b}_p^\top \xi_i + d_p - \mathbf{a}_p^\top \mathbf{x}}{\|\mathbf{b}_p\|_*} \right\}_{i \in [N]}$. Hence, it follows

$$s^* \leq \frac{q_p + d_p - \mathbf{a}_p^\top \mathbf{x}}{\|\mathbf{b}_p\|_*},$$

which leads to the satisfaction of (19d). ■

Proof of Theorem 1

proof By comparing $\mathcal{X}_{\text{SFLA}}(\boldsymbol{\kappa})$ in (22) and $\mathcal{X}_{\text{Exact}}$ through its equivalent and strengthened reformulation in (20), the proof is apparent due to the following inequality given $\kappa_i \in [0, 1]$ for all $i \in [N]$:

$$\left(\frac{\mathbf{b}_p^\top \xi_i + d_p - \mathbf{a}_p^\top \mathbf{x}}{\|\mathbf{b}_p\|_*} \right)^+ \geq \kappa_i \left(\frac{\mathbf{b}_p^\top \xi_i + d_p - \mathbf{a}_p^\top \mathbf{x}}{\|\mathbf{b}_p\|_*} \right).$$
■

Proof of Lemma 2

proof (23) \implies (16): Denote $-\widehat{\text{dist}}(\xi_i, \mathcal{S}(\mathbf{x}))$ by $v(\xi_i)$, and assume that s' is selected such that the term $s' + \frac{1}{\epsilon N} \sum_{i \in [N]} \max\{0, v(\xi_i) - s'\}$ is minimized. Then, take $r_i^* = \max\{0, v(\xi_i) - s'\}$ (implying $r_i^* \geq 0$). The inequality in (23) indicates the following:

$$\frac{\theta}{\epsilon} + s' + \frac{1}{\epsilon N} \sum_{i=1}^N r_i^* \leq 0 \Leftrightarrow \epsilon N s' + \sum_{i=1}^N r_i^* \leq -\theta N. \quad (27)$$

Taking $s^* = -s'$, now we will prove that the tuple $(\mathbf{x}, s^*, \mathbf{r}^*)$ satisfy all the constraints in (16), namely (15a)–(15c), for any \mathbf{x} belonging to the set (23). Since $r_i^* \geq 0$ and $-\theta N \leq 0$, (27) implies $s' \leq 0$ (i.e., $s^* \geq 0$) and the following inequality:

$$\epsilon N s - \sum_{i=1}^N r_i \geq \theta N,$$

which means (15a) and (15b) are satisfied. It remains to prove the satisfaction of (15c). Based on the setting of r_i^* , we have:

$$s^* - r_i^* = s^* - \max \{0, v(\xi_i) + s^*\} = s^* - \max \{0, s^* - \widehat{\text{dist}}(\xi_i, \mathcal{S}(\mathbf{x}))\}. \quad (28)$$

Notice that constraint (15c) is equivalent to:

$$\widehat{\text{dist}}(\xi_i, \mathcal{S}(\mathbf{x})) = \min_{p \in [P]} \left\{ \kappa_i \frac{\mathbf{b}_p^\top \xi + d_p - \mathbf{a}_p^\top \mathbf{x}}{\|\mathbf{b}_p\|_*} \right\} \geq s - r_i \quad \forall i \in [N]. \quad (29)$$

When $\widehat{\text{dist}}(\xi_i, \mathcal{S}(\mathbf{x})) \geq s^*$, (15c) must be satisfied for $(\mathbf{x}, s^*, \mathbf{r}^*)$ due to $r_i^* \geq 0$. When $\widehat{\text{dist}}(\xi_i, \mathcal{S}(\mathbf{x})) < s^*$, we have $s^* - r_i^* = \widehat{\text{dist}}(\xi_i, \mathcal{S}(\mathbf{x}))$ based on (28). Therefore, (29) and equivalently (15c) is satisfied.

(23) \iff (16): For any \mathbf{x} belonging to the set (16), by definition there exist (\mathbf{r}, s) such that constraints in the set (16), namely (15a)–(15c), are satisfied. Among these constraints, (15c) (equivalently (29)) informs that:

$$r_i \geq s - \widehat{\text{dist}}(\xi_i, \mathcal{S}(\mathbf{x})).$$

Combining with $r_i \geq 0$ in (15a), we further have:

$$r_i \geq \max \{0, s - \widehat{\text{dist}}(\xi_i, \mathcal{S}(\mathbf{x}))\}.$$

Then we have:

$$\epsilon N s - \sum_{i \in [N]} r_i \leq \epsilon N s - \sum_{i \in [N]} \max \{0, s - \widehat{\text{dist}}(\xi_i, \mathcal{S}(\mathbf{x}))\}.$$

Because of $\epsilon N s - \sum_{i \in [N]} r_i \geq \theta N$ in (15b), we have:

$$\epsilon N s - \sum_{i \in [N]} \max \{0, s - \widehat{\text{dist}}(\xi_i, \mathcal{S}(\mathbf{x}))\} \geq \theta N,$$

which means:

$$\frac{\theta}{\epsilon} - s + \frac{1}{\epsilon N} \sum_{i \in [N]} \max \{0, s - \widehat{\text{dist}}(\xi_i, \mathcal{S}(\mathbf{x}))\} \leq 0.$$

Now take $s' = -s$, we further have:

$$\frac{\theta}{\epsilon} + s' + \frac{1}{\epsilon N} \sum_{i \in [N]} \max \{0, -s' - \widehat{\text{dist}}(\xi_i, \mathcal{S}(\mathbf{x}))\} \leq 0$$

which leads to:

$$\frac{\theta}{\epsilon} + \min_{s'} \left\{ s' + \frac{1}{\epsilon N} \sum_{i \in [N]} \max \{0, -s' + v(\xi_i)\} \right\} \leq 0.$$

Therefore, the constraint in (23) is satisfied. ■

Proof of Lemma 3

proof Notice that the CVaR of a random variable $v(\boldsymbol{\xi})$ with $\boldsymbol{\xi} \sim \mathbb{P}_N$ in (24) can be equivalently expressed as the following optimization form:

$$\mathbb{P}_N\text{-CVaR}_{1-\epsilon}(v(\boldsymbol{\xi})) = \min_{s' \in \mathbb{R}, r \geq 0} s' + \frac{1}{\epsilon N} \sum_{i=1}^N r_i \quad (30a)$$

$$\text{s.t. } r_i \geq v(\boldsymbol{\xi}_i) - s', \quad i \in [N]. \quad (30b)$$

By strong duality of linear programming, we have:

$$\mathbb{P}_N\text{-CVaR}_{1-\epsilon}(v(\boldsymbol{\xi})) = \max_{\mathbf{0} \leq \mathbf{y} \leq \mathbf{1}} \frac{1}{\epsilon N} \sum_{i \in [N]} v(\boldsymbol{\xi}_i) y_i \quad (31a)$$

$$\text{s.t. } \frac{1}{N} \sum_{i \in [N]} y_i = \epsilon. \quad (31b)$$

Without loss of generality, assume that we have an ordering $v(\boldsymbol{\xi}_1) \geq \dots \geq v(\boldsymbol{\xi}_N)$. Then a primal-dual optimal pair for CVaR is given by:

$$s'^* = v(\boldsymbol{\xi}_{k+1}), \quad (32a)$$

$$r_i^* = \max\{0, v(\boldsymbol{\xi}_i) - s'^*\}, \quad (32b)$$

$$y_i^* = \begin{cases} 1, & i = 1, \dots, k \\ \epsilon N - k, & i = k + 1 \\ 0, & i > k + 1. \end{cases} \quad (32c)$$

The validity of the above primal-dual optimal pair holds because of the satisfaction of primal and dual constraints ($\mathbf{y}^* \in [0, 1]$ and $\mathbf{r}^* \geq 0$) and the equality of the objectives of the primal and dual problems:

$$\frac{1}{\epsilon N} \sum_{i \in [N]} v(\boldsymbol{\xi}_i) y_i^* = s'^* + \frac{1}{\epsilon N} \sum_{i \in [N]} r_i^*,$$

which holds because of:

$$\begin{aligned} \frac{1}{\epsilon N} \sum_{i \in [N]} v(\boldsymbol{\xi}_i) y_i^* &= \frac{1}{\epsilon N} \left(\sum_{i \in [k]} v(\boldsymbol{\xi}_i) + v(\boldsymbol{\xi}_{k+1})(\epsilon N - k) \right) \\ &= v(\boldsymbol{\xi}_{k+1}) + \frac{1}{\epsilon N} \left(\sum_{i \in [k]} v(\boldsymbol{\xi}_i) - k v(\boldsymbol{\xi}_{k+1}) \right) \end{aligned}$$

and

$$\begin{aligned} s'^* + \frac{1}{\epsilon N} \sum_{i \in [N]} r_i^* &= v(\boldsymbol{\xi}_{k+1}) + \frac{1}{\epsilon N} \sum_{i \in [N]} \max\{0, v(\boldsymbol{\xi}_i) - v(\boldsymbol{\xi}_{k+1})\} \\ &= v(\boldsymbol{\xi}_{k+1}) + \frac{1}{\epsilon N} \sum_{i \in [k]} (v(\boldsymbol{\xi}_i) - v(\boldsymbol{\xi}_{k+1})) \\ &= v(\boldsymbol{\xi}_{k+1}) + \frac{1}{\epsilon N} \left(\sum_{i \in [k]} v(\boldsymbol{\xi}_i) - k v(\boldsymbol{\xi}_{k+1}) \right), \end{aligned}$$

where the second equality holds because of our ordering of $v(\boldsymbol{\xi}_i)$ such that $v(\boldsymbol{\xi}_i) - v(\boldsymbol{\xi}_{k+1}) \leq 0$ for $i \geq k + 1$.

Now take $v(\xi_i) = -\widehat{\text{dist}}(\xi_i, \mathcal{S}(\mathbf{x}))$. Based on the CVaR interpretation of $\mathcal{X}_{\text{LA}}(\boldsymbol{\kappa})$ in (23) and the CVaR value expressed as (30a), for any $\mathbf{x} \in \mathcal{X}_{\text{LA}}(\boldsymbol{\kappa})$, we have:

$$\frac{\theta}{\epsilon} + \mathbb{P}_N\text{-CVaR}_{1-\epsilon} \left(-\widehat{\text{dist}}(\xi_i, \mathcal{S}(\mathbf{x})) \right) \leq 0 \quad (33a)$$

$$\Leftrightarrow \frac{\theta}{\epsilon} + s'^* + \frac{1}{\epsilon N} \sum_{i=1}^N r_i^* \leq 0 \quad (33b)$$

$$\Leftrightarrow \epsilon N s'^* + \sum_{i=1}^N r_i^* \leq -\theta N. \quad (33c)$$

Since $r_i^* \geq 0$ and $-\theta N \leq 0$, (33c) indicates $s^* := -s'^* \geq 0$ and

$$\epsilon N s^* - \sum_{i \in [N]} r_i^* \geq \theta N, \quad (34)$$

which means (15a) and (15b) are satisfied. It remains to prove the satisfaction of (15c). Based on the setting of r_i^* in (32b), we have:

$$s^* - r_i^* = s^* - \max\{0, v(\xi_i) + s^*\} = s^* - \max\{0, s^* - \widehat{\text{dist}}(\xi_i, \mathcal{S}(\mathbf{x}))\}. \quad (35)$$

Recall that constraint (15c) is equivalent to the following (see (29)):

$$\widehat{\text{dist}}(\xi_i, \mathcal{S}(\mathbf{x})) = \min_{p \in [P]} \left\{ \kappa_i \frac{\mathbf{b}_p^\top \xi + d_p - \mathbf{a}_p^\top \mathbf{x}}{\|\mathbf{b}_p\|_*} \right\} \geq s - r_i \quad i \in [N].$$

When $\widehat{\text{dist}}(\xi_i, \mathcal{S}(\mathbf{x})) \geq s^*$, (15c) must be satisfied due to $r_i^* \geq 0$. When $\widehat{\text{dist}}(\xi_i, \mathcal{S}(\mathbf{x})) < s^*$, we have $s^* - r_i^* = \widehat{\text{dist}}(\xi_i, \mathcal{S}(\mathbf{x}))$, so (15c) is satisfied as well. Therefore, we have proved that the pair $(\mathbf{x}, s^*, \mathbf{r}^*)$ satisfies constraints in (15) for any $\mathbf{x} \in \mathcal{X}_{\text{LA}}(\boldsymbol{\kappa})$, with $s^* = -s'^* = -v(\xi_{k+1})$ and $r_i^* = \max\{0, v(\xi_i) + s^*\}$. Finally, based on our ordering, $v(\xi_{k+1}) = -\widehat{\text{dist}}(\xi_{k+1}, \mathcal{S}(\mathbf{x}))$ is the $(k+1)$ -th greatest value amongst $\{v(\xi_i)\}_{i \in [N]}$, so $s^* = -v(\xi_{k+1})$ is the $(k+1)$ -th smallest value amongst $\{\widehat{\text{dist}}(\xi_i, \mathcal{S}(\mathbf{x}))\}_{i \in [N]}$. ■

Proof of Theorem 2

proof It is equivalent to prove that for any $\mathbf{x} \in \mathcal{X}_{\text{LA}}(\boldsymbol{\kappa})$, we have $\mathbf{x} \in \mathcal{X}_{\text{SFLA}}(\boldsymbol{\kappa})$, namely that constraints (21a)–(21d) can be satisfied. Based on Lemma 3, for any $\mathbf{x} \in \mathcal{X}_{\text{LA}}(\boldsymbol{\kappa})$ in (16), there always exists (\mathbf{r}^*, s^*) such that s^* is equal to the $(k+1)$ -th smallest value amongst the set $\{\widehat{\text{dist}}(\xi_i, \mathcal{S}(\mathbf{x}))\}_{i \in [N]}$ and constraints (15a)–(15c) are satisfied, which indicate the satisfaction of (21a)–(21c).

It remains to show the satisfaction of (21d) given the same (\mathbf{r}^*, s^*) . Without loss of generality, suppose that we have the following ordering $\widehat{\text{dist}}(\xi_1, \mathcal{S}(\mathbf{x})) \leq \dots \leq \widehat{\text{dist}}(\xi_N, \mathcal{S}(\mathbf{x}))$. Then denote its $(k+1)$ -th smallest element as $\widehat{\text{dist}}^*(\mathbf{x}) := \widehat{\text{dist}}(\xi_{k+1}, \mathcal{S}(\mathbf{x})) = s^*$. Based on (14), we have:

$$\widehat{\text{dist}}^*(\mathbf{x}) = \kappa_{k+1} \left(\min_{p \in [P]} \frac{\mathbf{b}_p^\top \xi_{k+1} + d_p - \mathbf{a}_p^\top \mathbf{x}}{\|\mathbf{b}_p\|_*} \right).$$

Then for any $p \in [P]$, when $i \geq k+1$, we have:

$$s^* = \widehat{\text{dist}}^*(\mathbf{x}) \leq \widehat{\text{dist}}(\xi_i, \mathcal{S}(\mathbf{x})) = \kappa_i \left(\min_{p \in [P]} \frac{\mathbf{b}_p^\top \xi_i + d_p - \mathbf{a}_p^\top \mathbf{x}}{\|\mathbf{b}_p\|_*} \right) \leq \kappa_i \left(\frac{\mathbf{b}_p^\top \xi_i + d_p - \mathbf{a}_p^\top \mathbf{x}}{\|\mathbf{b}_p\|_*} \right).$$

In other words, for any $p \in [P]$, there will be at least $N - k$ elements in the set $\{\kappa_i(\mathbf{b}_p^\top \boldsymbol{\xi}_i + d_p - \mathbf{a}_p^\top \mathbf{x}) / \|\mathbf{b}_p\|_*\}_{i \in [N]}$ not less than s^* . Since q_p is defined as the $(k+1)$ -th smallest value of $\{\mathbf{b}_p^\top \boldsymbol{\xi}_i\}_{i \in [N]}$, $(q_p + d_p - \mathbf{a}_p^\top \mathbf{x}) / \|\mathbf{b}_p\|_*$ is the $(k+1)$ -th smallest element of the set $\{(\mathbf{b}_p^\top \boldsymbol{\xi}_i + d_p - \mathbf{a}_p^\top \mathbf{x}) / \|\mathbf{b}_p\|_*\}_{i \in [N]}$. We can then deduce that $(q_p + d_p - \mathbf{a}_p^\top \mathbf{x}) / \|\mathbf{b}_p\|_*$ is not less than the $(k+1)$ -th smallest element of the set $\{\kappa_i(\mathbf{b}_p^\top \boldsymbol{\xi}_i + d_p - \mathbf{a}_p^\top \mathbf{x}) / \|\mathbf{b}_p\|_*\}_{i \in [N]}$ due to $\kappa_i \in [0, 1]$. Therefore, we must have:

$$s^* \leq \frac{q_p + d_p - \mathbf{a}_p^\top \mathbf{x}}{\|\mathbf{b}_p\|_*}$$

which indicates the satisfaction of (21d). \blacksquare

Proof of Corollary 1

proof Proposition 9 in Chen et al. (2023) demonstrates that the LA method can achieve an optimal value equivalent to the exact reformulation of RHS-WDRJCC by optimizing κ . We can then adjust the objective function $c(\cdot)$ and the set \mathcal{X} to identify each individual feasible solution $\mathbf{x} \in \mathcal{X}_{\text{Exact}}$, thereby establishing set equivalence. This set equivalence also applies to our proposed SFLA due to Theorem 2. \blacksquare

Proof of Corollary 3

proof Based on the definition of $[N]_p$, we have:

$$\mathbf{b}_p^\top \boldsymbol{\xi}_i \geq q_p, \quad \forall i \in [N] \setminus [N]_p, p \in [P]. \quad (36)$$

Therefore, the constraint (21d) in $\mathcal{X}_{\text{SFLA}}(\mathbf{1})$ implies that for any $i \in [N] \setminus [N]_p$ with $p \in [P]$, we have:

$$\frac{\mathbf{b}_p^\top \boldsymbol{\xi}_i + d_p - \mathbf{a}_p^\top \mathbf{x}}{\|\mathbf{b}_p\|_*} \geq \frac{q_p + d_p - \mathbf{a}_p^\top \mathbf{x}}{\|\mathbf{b}_p\|_*} \geq s. \quad (37)$$

As $r_i \geq 0$, we further have:

$$\frac{\mathbf{b}_p^\top \boldsymbol{\xi}_i + d_p - \mathbf{a}_p^\top \mathbf{x}}{\|\mathbf{b}_p\|_*} \geq s \geq s - r_i \quad (38)$$

which, combined with (21c) in $\mathcal{X}_{\text{SFLA}}(\mathbf{1})$, implies the satisfaction of (15c) when $\kappa = \mathbf{1}$. The above process implies $\mathcal{X}_{\text{SFLA}}(\mathbf{1}) \subseteq \mathcal{X}_{\text{LA}}(\mathbf{1})$. Combining with Theorem 2, we have $\mathcal{X}_{\text{SFLA}}(\mathbf{1}) = \mathcal{X}_{\text{LA}}(\mathbf{1})$. \blacksquare

Proof of Corollaries 4 and 5

proof The properties in Corollaries 4 and 5 hold for $\mathcal{X}_{\text{LA}}(\kappa)$ (16) as was proved from the perspective of the optimal value in Chen et al. (2023). This perspective can be extended to the whole set following our proof of Corollary 1, which in turn holds for our proposed SFLA $\mathcal{X}_{\text{SFLA}}(\kappa)$ due to Corollary 3. In fact, the first condition in Corollary 5 can be relaxed from $\forall \mathbf{x} \in \mathcal{X}_{\text{Exact}}$ to just the optimal solution \mathbf{x}^* , as the primary interest is typically in the optimal solution rather than the entire set. \blacksquare

C. Supplementary Information for the Unit Commitment Problems

C.1. Case Study Settings for the Unit Commitment Problem

The UC problem is implemented on the IEEE 24-bus network (Illinois Center for a Smarter Electric Grid (ICSEG) 1979). We set the number of gas generators in this network to be 100. The capacity of individual gas generators varies between 7.6 MW and 17.8 MW, and the total gas generation capacity is 1272 MW that follows the IEEE 24-bus test case data. The generator minimum uptime is set to 2 hours and the minimum downtime is set to 1 hour, representing

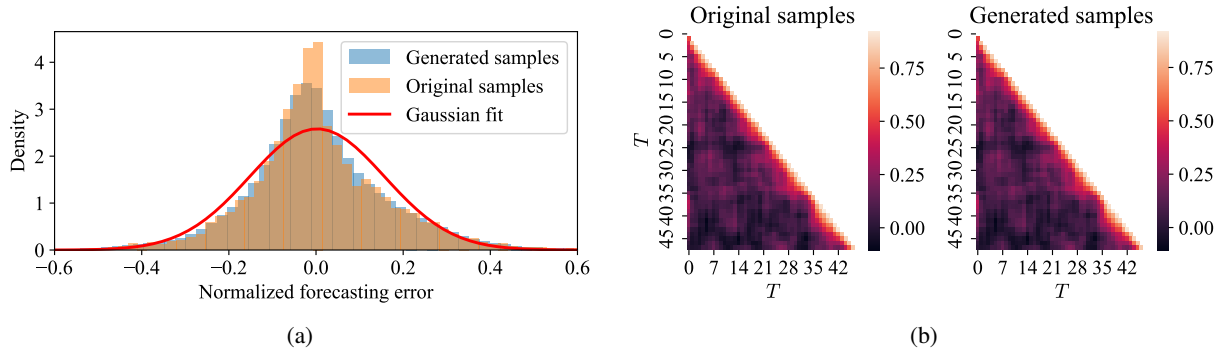


Figure 6 Comparison of original samples and generated samples for wind forecasting error.

Note. (a) The marginal distribution of the wind forecasting error, which is normalized by the wind generator capacity. Original samples are those 156 samples from Global Energy Forecasting Competition 2012 - Wind Forecasting, with each sample representing the next-48-hour forecasts. Generated samples refer to those generated by our fitted Gaussian KDE plus copula. We plot a Gaussian fit to highlight the non-Gaussian characteristic of both the original samples and the generated samples. (b) The temporal Pearson correlation coefficients.

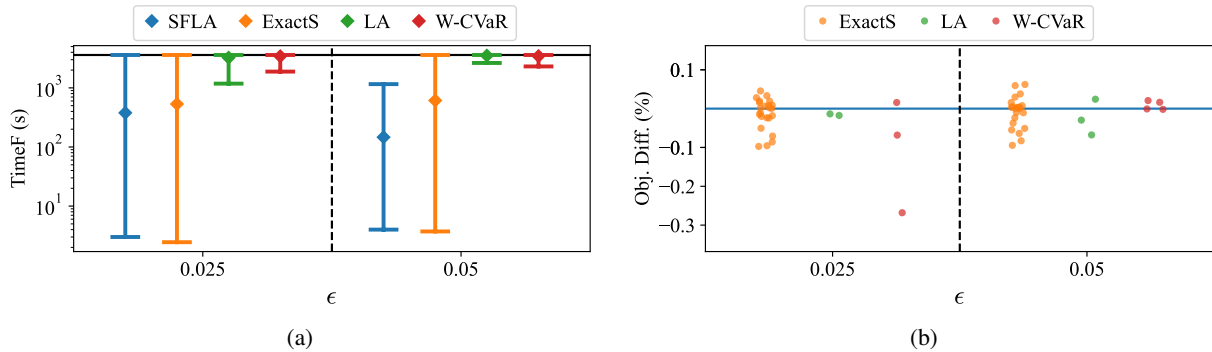


Figure 7 Performance comparison of the proposed SFLA with benchmarks for the UC problem: ExactS, LA, W-CVaR, and Bonferroni for the UC problem.

Note. The Wasserstein radius θ is set to 0.5 and the optimization horizon is set to $T = 24$. (a) Comparison of *TimeF* (s), where dots represent the mean value of the 30 random runs, with error bars indicating the 95% percentile interval (2.5th to 97.5th). The black horizontal line represents the one-hour *TimeLimit*. (b) Comparison of *Obj. Diff.* (%), where each dot represents the result for one of the 30 runs. The blue horizontal line indicates zero difference between the optimal value of a benchmark method compared to the proposed SFLA. Values higher than this horizontal line indicates that the benchmark achieves lower cost (better optimality) than the proposed SFLA. Note that we only keep certain random runs where the method to be compared and the proposed method are both solved to optimum. Many runs of LA and W-CVaR fail to solve to optimum and thus the plot only shows a few or zero dots for these two methods. The Bonferroni approximation is infeasible due to its over-conservativeness for all runs and is therefore not displayed.

gas turbines Xu et al. (2017). Other generator technical parameters follow Xu et al. (2017). We consider 10 wind farms with a total capacity of 730 MW, which is 60% of the total network load and represents a high level of renewable penetration. Following Yang et al. (2020), we consider uncertain wind power generation, which is modeled as a deterministic forecast plus a random forecasting error. Wind data, including forecasts and error samples, are obtained from open-access Bronze-medal forecasts (by Mudit Gaur) for the second wind farm in the Global Energy Forecasting

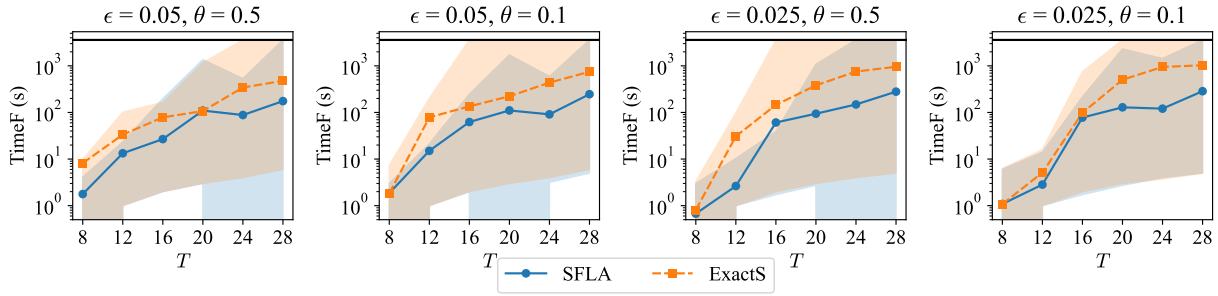


Figure 8 Computation time to obtain the first comparable high-quality solution under different optimization horizons T for the proposed SFLA and the benchmark ExactS for the UC problem.

Note. Dots represent the mean value of the 150 random runs, with shaded areas indicating the 95% percentile interval (from 2.5th to 97.5th). The black horizontal line represents the one-hour TimeLimit. The number of historical samples is set to $N = 100$.

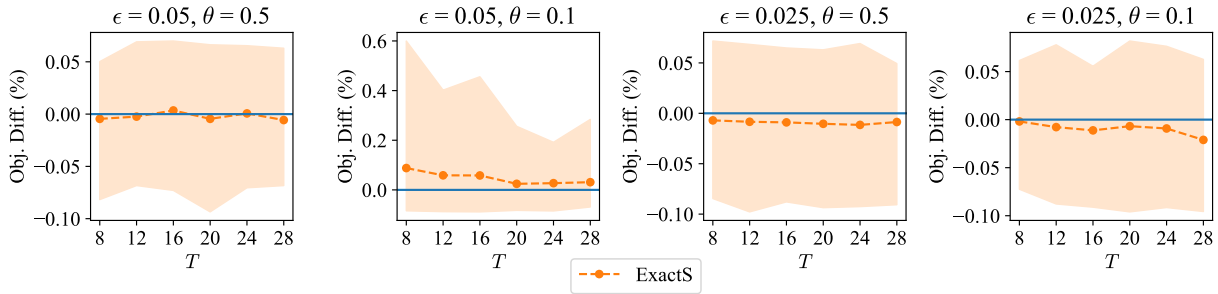


Figure 9 Comparison of optimality for different optimization horizons T for the proposed SFLA and the benchmark ExactS for the UC problem.

Note. The round dots represent the mean value of the 150 random runs, with error bars indicating the 95% percentile interval. The blue horizontal line indicates a zero difference of the optimal value of a benchmark method compared to the proposed SFLA. Values higher than this horizontal line indicates that the benchmark achieves lower cost (better optimality) than the proposed SFLA. The number of historical samples is set to $N = 100$.

Competition 2012 – Wind Forecasting (Hong et al. 2012). The competition task is to forecast the wind power generation for the next 48 hours based on real-world wind farm data. We take the out-of-sample forecasts from the Bronze-medal forecasting results, and then calculate the difference to the released ground-truth (Hong et al. 2014) to get 156 samples of wind power forecasting error, with each sample being the 48-hour forecasting error. These samples enable calculation of the temporal correlation matrix and the marginal distribution of the forecasting error. To enrich sample size while preserving the marginal distribution and temporal correlation, we utilize the Gaussian kernel density estimate (KDE) to fit the marginals and apply the Gaussian copula to generate temporally correlated samples that respect the marginal distribution. Figure 6 compares the original 156 samples and those generated by the Gaussian KDE plus copula, which show good fitting results that maintain the non-Gaussian marginal and the original temporal correlation.

To ensure robust conclusions, we conduct 30 random runs for each parameter setting of ϵ , θ , N , and T , increasing the number of random runs to 150 for specific evaluations when needed. In each random run, we:

1. Sample a distinct set of generator cost parameters from a uniform distribution based on the range suggested by Xu et al. (2017), which impacts the objective function of the UC problem.

2. Sample a different set of historical samples $\{\xi_i\}_{i \in [N]}$ for the random wind forecasting error, uniformly from a total of 1000 training data samples, which affects the feasible region of the UC problem.
3. Select a random starting simulation hour, uniformly sampled from the 24 hours of a day, which affects the demand and generation profiles and thereby alters the feasible region of the UC problem.
4. Set a different seed for the optimization solver, affecting the solver behaviors such as tie-breaking rules.

C.2. Supplementary Numerical Experiments of the Unit Commitment Problem

Figure 7a compares all methods with an optimization horizon $T = 24$. As can be seen, in terms of mean values, the proposed SFLA can have $4\times$ faster UC computation than the exact reformulation (ExactS) and even $20\times$ faster than the two linear approximation schemes, namely LA and W-CVaR. This demonstrates the computational efficiency of the proposed SFLA, and also the effectiveness of the strengthening process that makes ExactS even more computationally efficient than linear approximations. Figure 7b shows that the proposed SFLA has optimality comparable to ExactS and LA, where the minor difference of less than 0.1% is attributed to the preset 0.1% MIPGap. We also observed a random run of W-CVaR with a 0.25% worse optimality compared to the proposed SFLA, suggesting the higher conservativeness of W-CVaR. The Bonferroni approximation is infeasible for all cases because of its over-conservativeness. Overall, the observations above support both the computational gain and the approximation quality of the proposed SFLA.

Figures 8 and 9 compare the proposed SFLA and ExactS under progressively increasing optimization horizons T , a primary driver of problem complexity. Figure 8 shows that the proposed SFLA sustains its computational speedup as problem complexity increases. In contrast, the optimality differences illustrated in Figure 9 exhibit a flat or even decreasing trend for $(\epsilon = 0.05, \theta = 0.1)$. These results indicate that the proposed SFLA preserves computational efficiency in more complex cases without sacrificing optimality, making it particularly advantageous for practical high-complexity applications such as UC.

D. Supplementary Information for the Bilevel Bidding Problem

D.1. Case Study Settings for the Bilevel Bidding Problem

Our case study setting is based on the Alberta Case as described in Nasrolahpour et al. (2018). We have updated the storage efficiencies for both charging and discharging to 95%, in line with the setting in Zhou et al. (2021), which contrasts to Nasrolahpour et al. (2018) where discharging efficiency was overlooked. The original Alberta Case setup featured 14 generators. Given the complexity of bilevel optimization and the computational demands of the following intensive numerical simulations, we have selected only five generators (G2, G4, G6, G8, and G10). Then the capacities of these generators were scaled proportionally to achieve a combined capacity of 150% of the peak load (8768.89 MW), ensuring sufficient provision of generation and reserve. The modified maximum generation capacities for the five generators are 5248.98 MW, 2470.11 MW, 1482.07 MW, 1914.33 MW and 2037.84 MW respectively. Consistent with the UC case discussed in Section C.1, we incorporate uncertain wind generation, which is modeled as a deterministic forecast plus a random forecasting error. The total wind capacity is set to 4800 MW, which accounts for 60% of the total system load and represents a high level of renewable penetration. The wind data follows the UC case in Section C.1. We examine six time horizons $T \in \{4, 8, 12, 16, 20, 24\}$.

To ensure reliable conclusions, we conduct 30 random runs for each parameter setting of ϵ , θ , and T . In each random run, we:

Table 2 Comparison of the computation time for the bilevel problem

ϵ	θ	T	Time (s)				TimeF (s)			
			SFLA	LA	W-CVaR	Bonf.	SFLA	LA	W-CVaR	
0.05	0.01	4	6.83	430.86 (63.05×)	294.57 (43.10×)	0.08 (0.01×)	5.63	85.00 (15.09×)	91.67 (16.27×)	
		8	36.84	3200.45 (86.87×)	3332.34 (90.45×)	0.61 (0.02×)	29.63	666.80 (22.50×)	1244.39 (41.99×)	
		12	109.96	3600.03 (32.74×)	3355.00 (30.51×)	– (–)	66.20	1882.83 (28.44×)	2917.42 (44.07×)	
		16	371.21	3600.01 (9.70×)	3379.68 (9.10×)	– (–)	242.21	2916.23 (12.04×)	3600.00 (14.86×)	
		20	669.94	3600.01 (5.37×)	3600.06 (5.37×)	– (–)	562.13	3399.53 (6.05×)	3148.71 (5.60×)	
		24	1256.17	3600.01 (2.87×)	3600.08 (2.87×)	– (–)	933.50	3103.57 (3.32×)	3600.00 (3.86×)	
	0.05	4	7.73	332.43 (42.98×)	265.72 (34.35×)	– (–)	5.93	81.45 (13.73×)	103.09 (17.37×)	
		8	29.54	2595.57 (87.85×)	2906.47 (98.38×)	– (–)	24.97	554.10 (22.19×)	1139.05 (45.62×)	
		12	100.96	3572.06 (35.38×)	3279.78 (32.49×)	– (–)	56.73	2190.86 (38.62×)	2566.10 (45.23×)	
		16	462.03	3600.01 (7.79×)	3588.75 (7.77×)	– (–)	165.63	3240.63 (19.57×)	3542.70 (21.39×)	
		20	1013.09	3600.00 (3.55×)	3486.55 (3.44×)	– (–)	831.77	3461.63 (4.16×)	3203.17 (3.85×)	
		24	1249.38	3600.00 (2.88×)	3600.05 (2.88×)	– (–)	798.47	3519.83 (4.41×)	3386.57 (4.24×)	
0.025	0.01	4	2.55	75.94 (29.74×)	67.70 (26.52×)	0.34 (0.13×)	1.57	25.97 (16.57×)	29.15 (18.61×)	
		8	10.96	744.71 (67.97×)	454.49 (41.48×)	– (–)	8.93	134.24 (15.03×)	1679.56 (188.01×)	
		12	27.53	1633.57 (59.34×)	676.05 (24.56×)	– (–)	25.30	579.79 (22.92×)	305.33 (12.07×)	
		16	44.97	3074.33 (68.37×)	1643.78 (36.55×)	– (–)	39.73	1450.03 (36.49×)	1620.33 (40.78×)	
		20	73.87	3353.31 (45.39×)	1621.46 (21.95×)	– (–)	62.57	2320.12 (37.08×)	3600.00 (57.54×)	
		24	106.10	3573.18 (33.68×)	– (–)	– (–)	88.20	3180.79 (36.06×)	– (–)	
	0.05	4	3.39	39.35 (11.59×)	38.04 (11.21×)	– (–)	2.13	20.11 (9.43×)	17.68 (8.29×)	
		8	10.78	208.10 (19.31×)	139.15 (12.91×)	– (–)	9.53	85.57 (8.98×)	396.08 (41.55×)	
		12	16.75	609.51 (36.38×)	347.29 (20.73×)	– (–)	15.73	214.86 (13.66×)	324.00 (20.59×)	
		16	29.20	1293.95 (44.32×)	965.47 (33.07×)	– (–)	27.33	477.93 (17.49×)	842.50 (30.82×)	
		20	38.53	1960.49 (50.89×)	2035.01 (52.82×)	– (–)	36.27	981.31 (27.06×)	2007.50 (55.35×)	
		24	61.72	2240.78 (36.30×)	2705.43 (43.83×)	– (–)	50.20	1183.65 (23.58×)	2977.83 (59.32×)	

Entries with “–” indicate that no feasible runs were completed for that parameter setting. The *TimeF* (s) of Bonferroni approximation is not displayed because Bonferroni approximation is overly conservative such that it can easily find high *Bilevel Profit* (k\$) (the bilevel objective value) but poor *Actual Profit* (k\$) (plots 5d and 5l).

1. Sample a distinct set of generator bid prices from a uniform distribution ranging between 80% and 120% of the bid prices used by Nasrolahpour et al. (2018), which influences the objective function of the bilevel problem.
2. Sample a different set of historical samples $\{\xi_i\}_{i \in [N]}$ for the random wind forecasting error, uniformly from a total of 1000 training data samples, which affects the feasible region of the bilevel problem.
3. Select a random starting simulation hour, uniformly sampled from the 24 hours of a day, which affects the demand and generation profiles and thereby alters the feasible region of the bilevel problem.
4. Set a different seed for the optimization solver, affecting the solver behaviors such as tie-breaking rules.

D.2. Supplementary Analysis for the Bilevel Bidding Problem

A supplementary analysis of *Bilevel Profit* of the bilevel problem was conducted: among all 720 runs displayed in Figure 5, there are only three instances where *Bilevel Profit* of the proposed SFLA is slightly (less than 0.009 k\$) below that of LA and W-CVaR. This is caused by another aspect of numerical issue of the proposed SFLA that leads to an incorrect upper bound proved. Setting `NumericalFocus=3` of Gurobi effectively mitigates this issue. Compared to the numerical issue that renders the problem infeasible in LA and W-CVaR, the numerical issue associated with the proposed SFLA is minor.